國立臺灣大學醫學院分子醫學研究所

碩士論文

Institute of Molecular Medicine
College of Electrical Medicine
National Taiwan University

Master Thesis

Integrin βv與 Henji 在果蠅肌肉神經連結發育的角色探討

The roles of integrin βv and Henji during *Drosophila* neuromuscular junction development

王曼彧

Manyu Wang

指導教授：簡正鼎 博士

Advisor: Cheng-Ting Chien, Ph.D.

中華民國 100 年 7 月

July, 2011

Table of Contents

Abstract

In response to environmental and physiological stimulations or fluctuations, the synapse has to perform plasticity and also maintains homeostasis. Accumulating evidences support the role of the ubiquitin-proteasome system (UPS) in regulating synapse formation and remodeling, thus maintaining long-term neural circuit plasticity and homeostasis. Here we characterize the function of BTB-Kelch protein, the substrate receptor in the Cullin3 (Cul3)-organized ubiquitin E3 ligase, in the formation and neurotransmission of *Drosophila* neuromuscular junctions (NMJs). Mutant NMJs lacking *henji* activity show a dramatic increase in bouton number, including the appearance of numerous satellite boutons. Ultrastructurally, the electron-dense membrane area delineating the presynaptic active zone and the postsynaptic density (PSD) is expanded and the periactive zone is concurrently decreased in *henji* mutants. The PSD houses glutamate receptors (GluRs) IIA and IIB that show distinct transmissions at *Drosophila* NMJs. In *henji* mutants, the GluRIIA abundance is upregulated and the GluRIIB is downregulated. Our electrophysiological results also support a composition shift toward a higher GluRIIA/IIB ratio at *henji* mutant NMJs. By rescue experiments, we show that Henji acts in the postsynapse to regulate proper NMJ growth and GluRIIA/IIB composition.

We further show that Henji controls NMJ growth and GluRIIA/IIB ratio by

downregulation of dPak at PSDs. The postsynaptic dPAK marks the PSD area and regulates the GluRIIA abundance. Losing one copy of *dpak* suppressed the bouton phenotype and GluRIIA abundance in the *henji* mutant. Also, the intensity and area of dPAK punctates at PSDs were increased in *henji* mutants. We found that dPAK interacts with Henji, which promotes ubiquitination and degradation of dPak. Therefore, Henji acts at PSDs to restrict both the presynaptic bouton growth and the postsynaptic GluRIIA clustering via controlling dPAK protein level.

Several questions remain to be addressed: the subcellular localization of Henji; how dPAK is regulated by Henji during its activation; and how the GluRIIA/IIB balance is controlled by Henji-regulated dPak levels. Some preliminary results and future works will be presented in the thesis.

In addition, we also addressed the role of integrin βν in restricting NMJ growth. In the loss of βν activity, drastic increase in bouton number was observed. Further, we dissected the downstream signaling of βν/FAK56 and reported a bifurcating cascade of NF1-regulated cAMP/PKA and Vap-mediated Ras/MAPK pathways.

摘要

受到許多外生環境因子與內在生理刺激的種種刺激，突觸會調整其外部形態或內在的分子機制來應對，這種突觸的可塑性對於維持其功能甚至是神經網絡的恆定是不可缺的，而近來有越來越多的研究證據顯示泛素—蛋白質降解體系統(ubiquitin-proteasome system, UPS)在突觸的發育、重塑與維持神經迴路的穩定上扮演了重要的角色。在本篇研究裡，我們發現一個 BTB-Kelch 蛋白質(CG6224)對果蠅的神經肌肉鍵結發育與該突觸電生理功能的調控有很重要的影響，BTB-Kelch 這一類的蛋白質是存在於泛素的 E3 連結酶複合體(E3 ligase complex)中、連接支架蛋白 Cullin 與降解標的受質的一個蛋白質橋梁，因此又稱為受質受體(substrate receptor)。

一般的軸突末端會有一些樹枝狀的分枝，在這些分枝上會有一個個澎大突起的構造，稱為 varicosities 或 boutons，其形態就好像一個個珠子串在線上一樣，而缺乏此特定 BTB-Kelch 基因的果蠅突變株，其神經肌肉鍵結處的突觸型態與控制組有明顯不同：突變株的 bouton 數量增加很多，其中還包含了許多聚集在軸突分枝最末端的小型 boutons，這些 boutons 除了較小之外，它們分自兩個以上的分岔(multiple branch)，此現象與一般末端的雙分岔(double-branch)不同，呼應此突變株特別的表型，我們將此特定的 BTB-Kelch 蛋白質命名為「很擠」(henji)，除此之外，經由免疫螢光染色，我們分析了數種突觸的標記蛋白質(marker proteins)，結果發現後突觸緻密的一個激酶 dPak (Drosophila p21-activated kinase)染色範圍在突變株裡有增大的情況，而相對的側活化區標記蛋白質 FasII (FasciclinII) 訊號則減少了，電子顯微切片也可以看到在突變株的樣本中，bouton 邊緣電子緻密的範圍變長，這些證據顯示在缺乏 henji 的情況下，果蠅神經肌肉鍵結的突觸有型態上的缺失，包含了 bouton 數目與外型異常、活化區範圍變大而測活化區變小以及一些地域性的蛋白質如 dPak 有增量的趨勢。另一方面，隨著 dPak 在突觸區域的量增加，受其調控的谷氨酸受體 IIA (GluRIIA)的量也隨之增加，相反的，另一型的 GluRIIB 受體則減少，因此我們發現除了調控突觸的外

部型態外，Henji 也影響突觸上谷氨酸受體的組成，進而影響該突觸的電生理特性。

觀察到上述的表型，我們推測 henji 是經由負向調控 dPak 在突觸區域的蛋白量來限制該處 GluRIIA/GluRIIB 的比例，確實 dPak 的蛋白量在缺乏 henji 的果蠅中有全面性的增加，另外在果蠅的 S2 細胞中，表達 Henji 確實可以促進 dPak 受到多泛素標定(polyubiquitination)，從這些實驗我們確認了 dPak 是 henji 的降解目標蛋白。更進一步我們想知道 henji 突變株在神經肌肉鍵結突觸表現出的異常是否是因為 dPak 蛋白量過度累積所造成的，因此我們在 henji 突變株中減少一個基因量的 dPak，發現這樣可以使 GluRIIA 的量回復正常，同樣的，bouton 的數量與突變株相比也有部分的抑制。至於 Henji 是如何調控 dPak，詳細的分子機制目前仍未得出結論，這也是我們未來研究的目標之一。

在這篇研究的另一部分，我們也嘗試去定義 integrin βv在果蠅神經肌肉鍵結突觸發育過程中的角色，在 integrin βv的突變株中，bouton 的數量有顯著的增加，我們也描述了此受體調控 bouton 數量的詳細下游訊息傳遞路徑，其中包含 FAK (focal adhesion kinase)與兩個受其影響的 RasGAPs：(1) NF1 (neurofibromatosis1) 與受其控制的 cAMP 路徑 (2) Vap (vascular penduncle)與受其控制的 ERK-MAPK 路徑，此二訊息傳遞路徑皆受 integrin βv調控並且都參與突觸發育與 bouton 數量的控制。

Chapter 1. General Introduction

Synapses are highly dynamic structures that are subject to developmental cues for their assembly and maturation and are also modulated by neuronal activities throughout life. This extensive plasticity includes modulations of both morphology and neurotransmission properties. The former includes changes in synaptic size, shape and branching patterns; the latter is often perceived as alterations in protein synthesis, distribution, post-translational modifications and degradation (Nelson *et al*., 2003; Yi and Ehlers, 2005). We are especially interested in understanding mechanisms regulating synaptic growth and the role of ubiquitination in modulating synaptic physiologies.

The *Drosophila* neuromuscular junction (NMJ) has been employed as an accessible model synapse and has been studied intensively for decades (reviewed by Keshishian *et al*., 1996). The motoneuron axon terminals innervate body wall muscles with specified, stereotyped patterns which allow comparisons between individuals. At the contact sites, presynaptic nerve terminals branch and forms enlarged bulb-like structure named varicosities or boutons where neurotransmitter-containing vesicles aggregate and dock (Ruiz-Cañada and Budnik, 2006). Starting to form from late embryos, the NMJs undergo dramatic extension along with 10-100 folds of body muscle enlargement throughout three stages of larval development (Schuster *et al*., 1996). With the advantage of fly genetic tools and electrophysiological measurements, numerous

aspects of synapse biology have been described in the language of molecules.

The establishment of NMJs is regulated by transsynaptic developmental cues such as anterograde BMP/Gbb signaling and retrograde Wnt1/Wg pathway in order to coordinate pre- and post-synaptic growth (Collins and DiAntonio, 2007). Another phosphatidylinositol-4,5-bisphosphate/Wiscott-Aldrich syndrome protein (PI(4,5)P2/ WASP) signaling inhibits synaptic growth via cytoskeleton reorganization and is independent of BMP/Gbb pathway (Khuong et al., 2010). NMJ morphology and growth are highly sensitive to various developmental and environmental changes: increased neuronal activity by locomotion dramatically remodels and strengthens the NMJ (Sigrist et al., 2003). More pathways influencing synaptic growth in response to different physiological contexts are still waiting to be described.

The extracellular matrix (ECM) molecules secreted from neurons, muscle cells and glial cells accumulate in the synaptic cleft and bridges the pre- and postsynapse in both structural and signaling ways (Dityatev and Schachner, 2006). Integrins, one large family of transmembrane ECM receptors, are heterodimers comprised of one α and one β chains; combination of different α and β variants produces integrins with diverse properties (Geiger et al., 2001). Emerging interests has been dedicated to study the roles of integrin in the nervous system. Integrins are indispensable for the maintenance of activity-dependent synaptic plasticity as multiple

mice mutants with reduced expressions of α or β subunits showed impairments in neurotransmission, long-term potention (LTP) or paired-pulse facilitation (Chan et al., 2003; Chan et al., 2006). Regulations of these forms of synaptic strengthening are dependent on the phosphorylation, recruitment and rearrangement of glutamate receptors (GluRs) (Dityatev and Schachner, 2006). In addition to the activity-induced alterations in synaptic transmission, integrins are also involved in the regulation of structural plasticity since hypomorphs for position-specific integrins have overgrown synapses and are defective in functional transmission upon acute pharmacological treatments (Beumer et al., 1999; Rohrbough et al., 2000). However, compared with the postsynaptic GluR-reorganization function of integrins during synaptic strengthing, the detailed molecular basis underlying the activity-dependent structural plasticity of the NMJ is not well-elucidated.

As a well-established *Drosophila* model synapse, the glutamatergic NMJ is unlike to that of vertegrate and nematode's but instead shares many similar properties to the mammalian central nervous system excitatory synapse (Gramates et al., 1999; Featherstone and Broadie, 2000). Fly glutamate receptors (GluRs) are homologous to vertebrate AMPA (α-amino-3-hydroxy-5-methyl-4-isoxazolepropionic acid) and kainite receptors while NMDA (N-methyl-D-aspartate) receptor homologs dNR1 and dNR2 are only known to be expressed in the CNS (DiAntonio, 2006; Xia and Chiang, 2009).

Functional fly glutamate receptors are tetramers composed of three common subunits, GluRIIC, GluRIID, GluRIIE, and an additional subunit of either GluRIIA or GluRIIB (Qin *et al.*, 2005). GluRIIA- and GluRIIB-containing types of glutamate receptors differ mainly in their channel-opening kinetics; therefore, changes in the ratio of GluRIIA/GluRIIB can greatly influence the postsynaptic responses to neuronal activities (DiAntonio *et al.*, 1999; Marrus *et al*., 2004). GluRIIA-type of receptor is abundant at immature boutons, presenting a high GluRIIA/GluRIIB ratio. Along with the gradual maturation of the PSD, more GluRIIB subunits are recruited to the synaptic contacting site and the GluRIIA/GluRIIB ratio becomes balanced (Schmid et al., 2008). However, mechanisms underlying such development- dependent GluR subunit composition switch remain undetermined. Additional to developmental cues, synaptic growth is also shaped by neuronal activity. Overexpression of GluRIIA at the postsynapse results in a larger junctional quantal size and bigger NMJs with more boutons than wildtype controls while postsynaptic overexpression of GluRIIB reduces quantal size (DiAntonio *et al*., 1999; Sigrist *et al*., 2002).

Opposing to *de novo* protein synthesis, temporal-spatial specific protein degradation by the ubiquitin-proteasome system (UPS) has emerged as an additional yet indispensible mechanism to control key molecular components at the synapse in both development and plasticity aspects (Yi and Ehlers, 2005). Malfunctioning UPS is also

deeply involved in the pathogenesis of several notorious neurodegenerative diseases including Parkinson's, Alzheimer's, Huntington's, and Prion diseases (reviewed by Ciechanover and Brundin, 2003). Therefore, decoding the molecular mechanism of the UPS network is highly valuable for the search of future therapies. The UPS tags target proteins with ubiquitin (Ub) chains through a serial action of the ubiquitin-activating enzyme (E1), ubiquitin-conjugating enzyme (E2) and the ubiquitin ligase (E3). The polyUb-labeled proteins are subsequently recognized and degraded by the 26S proteasome. Substrate specificity is typically determined by the large and diverse population of E3 ligases: each of them recognizes certain subsets of target proteins and mediates the attachment of ubiquitin to these substrates. Among all the identified E3 ligases, a great understanding comes from studies of the Cullin-RING family. The SCF complex is the largest E3 family known so far and canonically it is composed of the scaffolding Cullin1 (Cul1), the E2-binding RING-finger protein Roc1, the adaptor Skp-1 and the substrate-binding F-box protein. The E3 ligase complex binds the Ub-loaded E2 and F-box protein that recruit substrates at the same time. By bringing them in close proximity, Ub is transferred from E2 to the bound target. Specificity of ubiquitination by a particular SCF depends on the recognition of substrates by F-box proteins (reviewed by Deshaies, 1999). Cul1-containing SCFs recognizes distinct subsets of proteins targets from Cul3-containing ones. Regardless to the structural

similarity with conventional Cul1-based SCFs, Cul3 recruits BTB-containing proteins as substrate receptors (Geyer *et al*., 2003; Furukawa *et al*., 2003). The Drosophila genome encodes 60 BTB proteins and nine of which contain conserved Kelch-repeats. The N-terminal BTB domain binds to Cul3 and the C-terminus Kelch-repeats recognize ubiquitination targets, making these proteins substrate receptors of the Cul3 E3 ligase complex.

In the first part of study, our lab has done a series of genetic interactions and demonstrated that integrin βν specifically interacted with focal adhesion kinase (FAK56) in the regulation of NMJ growth (Tsai et al., 2008). Here we characterized the phenotypes of *βν* mutant and found it plays a critical role in inhibiting NMJ elaboration. Being activated and transducing the extracellular cue from βν receptor, we further revealed a bifurcating signaling downstream of FAK56, including Neuorfibromatosis 1 (NF1)-activated cAMP/PKA pathway and Vacuolar peduncle (Vap)-activated ERK/MAPK pathway. Both signalings are required for integrin αPS3βν to restrain unnecessary synaptic growth.

In the second part, a conserved BTB-Kelch protein, named as Henji, had been previously identified by our lab to cause overgrown NMJs featured with numerous, crowded satellite boutons. *Drosophila* p21-activated kinase (dPak), a kinase required for the clustering of GluRIIA at the postsynaptic membrane, was found to be a

ubiquitination substrate for Henji-Cul3 E3 ligase complex. In the absence of Henji, overall dPak protein accumulates and the protein levels at the NMJ were also elevated. Along with the enhanced dPak clustering, GluRIIA abundance was also increased as expected. When the phosphor-mimicking, constitutive-active form of dPak was overexpressed in the muscle, synaptic GluRIIA abundance was not altered. However, when this constitutively active form of dPak was postsynaptically overexpressed in *henji*$^{+/-}$ background, the intensity of GluRIIA punctae was significantly augmented as compared to heterozygous control and *henji*$^{-/-}$ mutant. This result showed that dPak protein level near the synaptic contact sites needed to be tightly controlled which critically modulated local GluRIIA balance. Our study provides evidences for spatial protein level regulation at subsynaptic sites by the UPS and this regulation is tightly associated with the electrophysiology properties of the synapse.

Chapter 2. Integrin βv/FAK56 negatively regulate *Drosophila* NMJ growth via bifurcating signaling cascade

2-1. Integrin βv is required for restraining bouton growth but not for the assembly of NMJs.

To understand the function of integrins at NMJs, the gross morphology was examined by co-immunostaining for horseradish peroxidase (HRP) labeling presynaptic membranes and Synapsin (Syn) marking presynaptic vesicles. Boutons were defined as bulged structures positive for both HRP and Syn and total bouton number from NMJ6/7 was quantified and normalized to its muscle area. Wall-climbing third instar larvae from wildtype and βv^{1} were compared. Two sets of NMJs: NMJ6/7 and NMJ4 were analyzed for a general observation. The NMJ6/7 contains complex branching and numerous boutons innervated by two motoneurons. Only NMJ6/7 from abdominal segment A3 hemisegments were used, regarding the slight morphological differences between segments. NMJ4 represents a simple, Y-shaped axon terminal having less boutons and lower-order branching than NMJ6/7; the NMJs look similar between segments and thus A2 to A6 segments were recorded. The most striking feature of βv^{1} mutant NMJ was the overelaborated axon terminals from both NMJ6/7 and NMJ4 (Figure1A, B). Loss of βv activity caused a 30% increase in total bouton number (Figure1C. w^{1118}, 13.00, n = 20;

βv^1, 17.18, n = 18, $p < 0.05$ by student t-test). Detailed examination of the synapse structures by immunostaining also showed no significant difference between mutant and wildtype (data not shown). Ultrastructural analysis by electron microscope (EM) showed no significant differences between βv^1 mutant and wildtype control (Figure 1 D, E). Our observation supported previous reports studying multiple integrin mutants that βv also plays as a negative regulator on synaptic growth at fly NMJs.

2-2. Integrin βν is required for synaptic growth regulation

With the aid of the tissue-specific UAS-GAL4 gene expression system, it is possible to differentiate the requirement of a gene in pre- or postsynaptic comportments of the synapse. We were interested to know whether βv performs its growth-restricting function in the neuron or in the muscle cell. Therefore, UAS transgene of βv was cloned and transgenic flies generated. I tried to rescue the $\beta v^1/\beta v^2$ transheterozygous mutant by expressing the *UAS-*βv transgene in either pre- or postsynapse using tissue-specific GAL4 drivers. Only expression of βv in the presynaptic compartment with pan-neuronal *elav-GAL4* driver fully rescued the overgrown NMJ found in $\beta v^1/\beta v^2$ mutant (Figure2). On the other hand, expression of *UAS-*βv with muscle-specific *MHC-GAL4* had no rescuing effect and the bouton numbers were similar to those from $\beta v^1/\beta v^2$ mutant NMJs (Figure2).

2-3. Integrin βν suppresses NMJ growth via regulating RasGAP activities

The bouton over-addition and nearly intact synapse structure of *βν* phenocopied the loss of *FAK*56 (the *Drosophila FAK* gene), which was characterized by a previous work from our lab (Tsai et al., 2008). In this study, losing one gene copy of *βν* caused significant bouton number increase when combined with the hypomorphic *FAK56* allele (*FAK56*$^{N30/KG}$), while either *βν*$^{+/-}$ *or FAK56*$^{N30/KG}$ did not alter bouton number. Among the complex signaling network downstream of integrin, this strong genetic interaction suggested that FAK may be responsible for regulating synaptic growth. Further, the accumulation of diphosphorylated ERK staining and reduced FasII signal at the NMJ proposed that FAK56 may regulate synaptic growth by inhibiting ERK activity.

To begin with, we tempted to clarify the downstream signaling players of the βν/FAK56 cascade; hypothesis was FAK56 may inhibit ERK phosphorylation by activating RasGAPs. All three *Drosophila* RasGAPs, namely, NF1, GAP1 and Vap, were tested for genetic interaction with *FAK56*$^{N30/KG}$ hypomorph (Appendix 1). Introducing one copy of *NF1*^{E2} null allele into *FAK56*$^{N30/KG}$ background induced dramatic bouton increase; heterozygous *NF1*^{E2} mutant alone did not alter total bouton number. Similarly, one copy of *vap*^{1} mutant allele combined with *FAK56*$^{N30/KG}$ also showed extensive bouton addition phenotype. GAP1 in contrast did not have noticeable genetic interaction with *FAK56* hypomorph in the regulation of NMJ growth. Therefore, FAK56 shows selective

genetic interacts with two RasGAPs, NF1 and Vap but not GAP1, to influence bouton addition. We then turned to dissect the functions and molecular mechanisms of NF1 and Vap at the synapse individually.

2-4. The integrin βν/FAK56 cascade regulates synaptic growth through cAMP/PKA pathway

NF1 is reported to regulate two parallel signaling pathways: Ras/MAPK and cAMP/PKA via its GAP and adenylate cyclase activation activities respectively (reviewed by Shilyansky et al., 2010). Studying specific *NF1* mutants has revealed that lacking of NF1 GAP activity results in disrupted circadian rhythm (Williams et al., 2001) and reduced larval/pupal length and adult wing area (Walker et al., 2006) and both circadian rhythm and body size control are dependent on the Ras/MAPK. On the other hand, as an activator for adenyl cyclase, NF1 positively regulates *Drosophila* longevity--NF1 mutant flies have shortened life span and this can be rescued or even prolonged by overexpressing PKA (Tong et al., 2007).

To figure out which signaling is involved in synaptic bouton growth regulation mediated by NF1, we asked and were grateful to receive various NF1 transgenic flies from Dr J. Walker. At first, I tried to confirm GAP activity is important for NF1 to regulate fly body size. I re-expressed rescue the $NF1^{E2}$ mutant pupae by wild-type, full-length NF1

transgene (hs-NF1 wt) or NF1 carrying point mutations (hs-NF1 RP and hs-NF1 KA) disrupting its GAP activity. The RP mutant substitute the arginine 1320 residue in the critical GRD finger loop for a proline(Scheffzek et al., 1997) and the corresponding human R1276P point mutation found in some neurofibromatosis patients has been shown to have more than 1000-fold reduction in the protein's GAP activity (Klose et al., 1998; Sermon et al., 1998); the replaced lysine1481 in KA mutant did not map within or close to the catalytic site but instead interfere with the binding affinity for Ras (Ahmadian et al. 2003). After 30 minutes of heat-shock every 24 hours until pupae were formed, wildtype NF1 expression almost completely restored $NF1^{E2}$ pupal size back to wildtype level. On the contrary, NF1 carrying KA or RP mutations or NF1 with truncated GAP-related domain (GRD) failed to rescue and showed reduced body lengths as in $NF1^{E2}$ (Figure 4A). Alternatively, I also overexpressed the GRD of NF1 alone in the presynapse and confirmed that this domain was sufficient to rescue pupal length of $NF1^{E2}$ null mutant as reported. Presynaptic introduction of NF1 GRD harboring KA also recued mutant pupal length while NF1 GRD RP did not (Figure 4B). It seemed the GAP activity of NF1 is both required and sufficient to regulate fly body size and its partial activity is sufficient for this control.

To understand the importance of the GAP activity of NF1 in regulating NMJ bouton growth, I firstly overexpressed either wildtype NF1 GRD or GRD RP in the presynapse

of $NF1^{E2}$. NMJ morphology was examined by immunostaining and bouton number was quantified. Surprisingly, both NF1 GRD wt and GRD RP failed to rescue the bouton overgrown phenotype in $NF1^{E2}$ (Figure 5). On the other hand, heat-shock overexpression of all full-length NF1 wt, NF1 KA or NF1 RP rescued the over-sprouted boutons to wildtype level (data by Tsai, not shown). These results demonstrated the GAP activity was not required for NF1 to suppress synapse growth at the NMJ.

Additional to RasGAP activity, NF1 can possibly regulate synaptic growth through activating cAMP/PKA signaling. To prove the hypothesis, I fed $NF1^{E2}$ flies with dibutyl cAMP (di-cAMP, a cell-permeable, less rapidly metabolized cAMP analog) or forskolin (a direct activator of adenylyl cyclase) to to see whether this manipulation on cAMP level can bypass the loss of *NF1*. $NF1^{E2}$ NMJs had excess boutons while the same mutant flies fed with di-cAMP or forskolin had normal number of boutons (Figure 6). di-cAMP and forskolin feeding similarly suppressed $FAK56^{N30/K24}$ mutant and βv^{1} bouton overgrowth (Figure 6 and Appendix 2). From the above results, we understand that βv/FAK56/NF1 signaling axis modulates NMJ bouton addition with cAMP-dependent mechanism.

2-5. The integrin βv/FAK56 cascade regulates synaptic growth through ERK/MAPK pathway

Another candidate involved in FAK-mediated bouton growth restriction was RasGAP Vap. NMJ morphology from *vap* mutants was firstly examined. Regardless to the grossly normal synapse structure, boutons increased significantly in both vap^{1} and vap^{2} (Figure 7) as seen in βv^{1} (Figure) and $FAK56^{N30/K24}$ (Tsai et al., 2008). Noteworthily, as a gene localized on X chromosome, only male *vap* larvae had overgrown boutons but NMJs from female homozygous mutant were quite normal in total number of boutons (Figure7). The molecular reason underlying this phenomenon was not clear. Considering this special prerequisite, only male larvae from *vap* mutants were used in all the following experiments.

To further understand whether the *vap* mutant NMJs were constructed appropriately, several pre- and postsynaptic markers were immunostained and analyzed. Bruchpilot (Brp) stained specialized vesicle release structures known as T-bars. Brp formed punctae at AZs and signals from vap^{1} appeared normal in both intensity and distribution (Figure 8A). Futsch, a microtubule associated protein, showed strong, continuous staining within axonal terminals and loop structure were found in some terminal boutons, which were stereotyped in wildtype (Figure 8B and data not shown). Discs large (Dlg) as a large scaffold protein required for the assembly of the postsynapse formed a halo surrounding the HRP-labeled neuronal membrane. Both intensity and thickness were similar between vap^{1} and wildtype (Figure 8C). *Drosophila*

p21-activated kinase (dPak) decorated each postsynaptic density (PSD) in a punctuate fashion (Figure 8D) and no obvious differences in punctuated pattern, punctae size or intensity were found in the lack of *vap*. Lastly, glutamate receptor subunit IIA (GluRIIA) was also scrutinized and its distribution and clustering in each PSD were quite normal (Figure 8E)

FascilinII (FasII), a NCAM-like adhesion molecule localized both pre- and postsynaptically, adheres and helps assemble the synapse via homophilic interaction (Sone et al., 2000). Local abundance of FasII at the NMJ is regulated by Ras-activated ERK/MAPK pathway and certain degree of reduction in FasII level promotes bouton addition during activity-dependent plasticity (Koh et al., 2002 The Ras1-MAPK signal transduction pathway regulates synaptic plasticity through fasciclin II-mediated cell adhesion. J Neurosci 2002, 22:2496-2504; Schuster et al., 1996). Considering the bouton overgrown phenotype *vap* mutants, I also analyzed and quantified FasII level at the NMJ. As expected, FasII intensity was reduced in vap^{1} when to wildtype (Figure 9A). Moreover, to know the degree of FasII reduction, I quantified its staining intensity. The intensity of FasII from a single branchlet containing 4 to 5 boutons were averaged and normalized to the HRP intensity from the same area. Results show local levels of FasII decreased about 20% (Figure 9B) and this decrease corresponded to the increase of bouton number (Figure 7).

UAS-RasGAP transgene was expressed in presynapse and and turned out to rescue the excess bouton phenotype in *vap*^{1} mutant (Figure10), suggesting a presynaptic requirement of Vap in regulating bouton growth.

Chapter 3. Characterization of *Henji*: results by Tze-Ting Lai, Pei-I Tsai, Ying-Ju Chen and Hsiu-Hwa Kao in the Chien lab

3-1. *henji* mutants

To understand the functions of Henji in synapse development and plasticity, loss-of-function *henji* mutants were generated. Firstly, the P-element insertion *BG01766* (Appendix 3A) was excised to generate the *C8-2* line that includes 1670 bp deletion, truncating parts of the 5' UTRs of *CG6169* and *CG6224* (which is named *henji* to describe its NMJ phenotypes). Mutants homozygous for the *C8-2* allele was embryonic lethal and the lethality could be rescued by introducing the *CG6169* genomic rescue construct (*CG6169-GR*). The *C8-2* chromosome carrying *CG6169-GR* was referred to as the $henji^{1}$ allele. The P-element line *PB{04604}*, inserted in the 5'UTR of *henji*, was named as $henji^{2}$ in this study. Both alleles were tested for expressions of Henji protein by immunoblotting with anti-Henji antibodies (Appendix 3B). Lane 1 to 3 and lane 6,7 were prepared form wall-climbing third instar larvae. Lane 1 showed endogenous Henji expression in w^{1118} control larvae. Lane 2 showed almost completely abolished Henji protein in the $henji^{1}$ mutant. Reintroduce henji gemonic rescue rescued about 80% of endogenous expression in $henji^{1}$ mutant. Lane 7 showed a significantly reduced Henji expression but still had some faint signal left in the $henji^{2}$ mutant compared to lane 6.

Lane 3 and 4 were extracted from S2 cell lysates. Lane4 showed strong endogenous Henji expression. Henji overexpression in Lane 5 showed a saturated band at the predicted molecular weight and some strong signals from higher molecular weight product, suggesting potential posttranslational modifications. These results are consistent with that *henji*^{1} is a near null allele and *henji*^{2} is a hypomorphic allele.

Although both *henji*^{1} and *henji*^{2} flies survived to the adult stage, they were found dead in the food several days after eclosion with no obvious morphological defects. Indeed, *henji*$^{-/-}$ flies had difficulties in climbing and walking and the larvae also move more sluggishly than normal individuals, hinting potential disability in locomotion ability. We therefore examined any defect in the larval NMJ.

3-2. *henji* mutant has abnormally expanded active zones

In wildtype NMJs, synaptic boutons decorate the presynaptic terminal process with simple branches in a beads-on-a-string pattern (Appendix 4A, C). NMJ morphology was revealed by co-immunostaining for HRP and Synaptotagamin (Syt) marking synaptic vesicles. Strikingly, *henji*$^{-/-}$ mutants displayed dramatically overgrown NMJs with supernumerary boutons (Appendix 4. controls, 56.5 ± 2.34, n = 26; *henji*^{1}, 101.7 ± 5.07, n = 24) and small satellite boutons (controls, 2.7±0.48, n=26; *henji*^{1}, 30.14±2,57, n=24) that are defined as small protrusions emanating from the primary axial branch of nerve

terminals (Dickman *et al.*, 2006). Impressed by this unrestrained bouton addition phenotype, we named this mutant 'Henji', indicating overcrowdedness in Chinese.

To gain insight into the detailed structural aberration of *henji* mutant NMJs, synaptic marker proteins were stained and analyzed for their expression levels and subcellular localization. The Brp pattern was normal in size, level and distribution in the *henji* mutant; however, the total punctae number in a single NMJ increased by about 25% as compared to wildtype (Appendix 5A, B), showing an overall increase in total vesicle release sites. On the postsynaptic side, PSDs revealed by dPak staining showed striking augment in both intensity and patch area in *henji*^{1} (Appendix 5A, C, D). However, these enlarged PSD patches were still membrane-localized and had normal apposition to presynaptic active zone labeled by Brp in single section images. The enlarged dPak patches hinted that AZs may be abnormally expanded in the lack of *henji*. Consistent with this presumption, peri-active zone area marked by FasII staining was drastically reduced and the remaining FasII signal occasionally overlapped with dPak patches, a phenomenon rarely found in wildtype boutons (Appendix 5E). Taken together with the upregulation of dPak, these results suggest the area of AZs is enlarged and the boundary between AZ and PAZ becomes ill-defined in *henji* mutant.

We further confirmed these NMJ defects by performing transmission electron microscopy (TEM). In *henji*^{1} NMJ sections, active zones were increased both in number

(control, 4.00 ± 0.37, n = 17; *henji*^{1}, 4.72 ± 0.25, n =43) and in length (control, 0.64±0.03, n=17; *henji*^{1}, 0.75±0.03, n=43) while average bouton perimeter was only slightly reduced (Appendix 6; control, 7.61±0.84, n=17; *henji*^{1}, 7.88±0.49, n=43). Regardless of the abnormalities in active zone area, synaptic vesicle size, distribution and density appear comparable between mutant and control boutons. The ultrastructural analysis supports the idea that AZ is expanded and the PAZ was concurrently reduced at NMJs lacking *henji* activity, suggesting that Henji has a role in regulating the size of active zones during synaptogenesis.

3-3. Henji interacts with dPak and promotes its degradation via the ubiquitin -proteasome system

Considering the elevation of dPak in PSDs and Henji being an adaptor protein for ubiquitin E3 ligase, we wondered that dPak might be a substrate ubiquitinated by the Henji-Cullin E3 complex. To test this hypothesis, the *dpak*^{6} null allele (homozygous *dpak*^{6} animals are embryonic lethal) introduced into *henji*$^{-/-}$ and the bouton phenotypes were evaluated. With one copy of *dpak* removed, the number of boutons found in *henji* mutant was reduced to the wildtype level and the appearance of supernumerary satellite boutons was also strongly suppressed (Appendix 7). The suppression of *henji* phenotype by reducing *dpak* activity is in consistence with the role of Henji in downregulating

dPak protein levels.

We then tested whether Henji functions as a ubiquitin ligase for dPak degradation. In *Drosophila* S2 cells transfected with *henji* dsRNA that depleted Henji expression, the dPak protein level was increased. Lysates prepared from larval body wall muscles of *henji*$^{-/-}$ had increased levels of dPak as well. As a control, the *Drosophila* Wnt1/Wg receptor Frizzled (dFz) expression remained unaltered in *henji*$^{-/-}$ mutant lysates (Appendix 8A, B). We then tested whether Henji promotes the ubiquitination of dPak in S2 cells by transfecting S2 cells with plasmids expressing Flag-Henji, Myc-dPAK and/or HA-Ub. In the presence of Henji, polyubiquitination of dPak was increased, as compared to that without ectopic expression of Henji (Appendix 8C). The BTB domain-containing substrate receptor is recruited by Cul3 to form a functional E3 Ub ligase Further analysis reveals interactions between dPak and both Henji and Cullin3 and the later interaction is impaired in Henji8A, a mutant with its Cullin-interacting ability abolished (Appendix 8D, E).

3-4. dPak regulats postsynaptic glutamate receptor abundance and accounts for the alterations in mEJP amplitude.

Glutamate receptor IIA (GluRIIA) clustering at PSDs requires synaptically localized dPak. In *dpak* null mutants, GluRIIA abundance at the NMJ is dramatically diminished

(Albin and Davis, 2004). Consist with an increase in dPak levels and patch size, GluRIIA intensity was greatly increased in *henji* mutants while the cluster size and number appeared normal (Appendix 9A). On the contrary, GluRIIB abundance was reduced in *henji*$^{-/-}$ mutants, representing a competing relation between these two GulR subunits (Appendix 9B).

We then tested whether overexpression of Henji was sufficient to downregulate dPak levels. When Henji was overexpressed in the muscle using C57-GAL4, dPak protein at the PSD was dramatically reduced, accompanied with decreased GluRIIA levels. In addition, the bouton became enlarged and the number was also decreased (Appendix 9C and data not shown), opposite to *henji* mutant phenotypes. These results suggest that Henji regulates dPak levels in the postsynapse of the NMJ.

To understand whether *henji* mutations alter the physiological responses, we measured the electrophysiological properties at the *henji* mutant NMJ. No obvious alteration was found for EJP (excitatory junctional potential) amplitude (Appendix 10A, B). However, a significant increase in mEJP (miniature excitatory junctional potential) was recorded (Appendix 10C, D), coinciding with the increased GluRIIA/GluRIIB ratio (since the presynaptic vesicle size and number were not significantly changed according to TEM data) in *henji* mutants. The frequency of mEJP was comparable to wildtype, consistent with intact presynaptic vesicle release machinery as seen in TEM sections. On the other

hand, the quantal content, calculated as the EJP amplitude divided by the mEJP amplitude, was decreased in the *henji* mutant (Appendix 10F), implying homeostatic compensation responsive to the augmented postsynaptic sensitivity in *henji* mutants. In addition, the NMJ of the *henji* mutant displays a larger decay time constant than control (data not shown), further confirming a glutamate receptor field composed of more slowly decayed GluRIIA and less rapidly decayed GluRIIB.

3-5. Henji functions at the postsynapse to regulate both presynaptic bouton growth and postsynaptic dPak protein levels

With effects in presynaptic bouton growth and postsynaptic dPak degradation by *henji* mutations, we then asked where Henji functions. Full-length *henji* cDNA was expressed presynaptically with *elav-GAL4* or postsynaptically with *C57-GAL4* in the *henji* mutant background. Postsynaptically expressed Henji rescued both bouton number and satellite bouton phenotypes found at *henji* mutant NMJs (Appendix 11D-F). However, neuronal expression of Henji failed to suppress the overgrown boutons (Appendix 11A-C), suggesting that Henji controls synaptic growth at the postsynapse. Therefore, some unidentified retrograde signaling is presumably to be involved in this transsynaptic regulation.

Chapter 4. The BTB-Kelch protein Henji promotes dPAK degradation to regulate synaptic growth and Glutamate receptor composition at *Drosophila* NMJs

4-1. Henji functions in the postsynapse to regulate GluRIIA abundance

Given that Henji function in postsynapses ie n regulating postsynaptic dPak levels and presynaptic bouton growth, we further tested t , while presynaptic expression of Henji failed to do so. To further test whether postsynaptic Henji activity also regulates NMJ physiology, the GluRIIA abundance were examined in *henji* mutants with pre- or postsynaptic expression of Henji. The intensity of membrane GluRIIA staining is comparable to wildtype when Henji is overexpressed postsynaptically in *henji*$^{-/-}$ background. On the contrary, GluRIIA punctae intensity of the presynaptic rescued NMJs is not significantly different from the *henji* mutant (Figure 1A). Electrophysiological analysis also shows a restoration of mEJP amplitude recorded from postsynaptically rescued NMJs but not presynaptically rescued ones (Figure 1B). These data suggest Henji's role in regulating NMJ growth and development is most importantly at posysynaptic sites.

4-2. Henji regulates GluRIIA abundance via dPak

Our previous data indicates that dPak is a degradation substrate of Henji-Cullin3

ubiquitination E3 ligase complex. In addition, we have shown that Henji regulates presynaptic bouton growth via downregulating dPak (Appendix 9). I further check whether reducing one copy of *dpak* gene can also rescue GluRIIA accumulation in *henji* mutant. This speculation comes from the report stating dPak is required for GluRIIA clustering at the NMJs (Albin and Davis, 2004). Similarly, I introduce one copy of $dpak^{6}$ null mutant allele into $henji^{-/-}$ flies and stained GluRIIA for analysis. Like presynaptic boutons, postsynaptic GluRIIA punctae intensity at the synapse is restored to levels close to wildtype after *dpak* gene dosage reduction (Figure 2). We then conclude that the elevation of GluRIIA abundance in *henji* mutants is an outcome of impaired dPak degradation in the lack of Henji and that dPak is an important substrate for Henji to regulate NMJ functions at both sides of the synapse.

4-3. Henji promotes dPak downregulation regardless to its active state

Mammalian Paks can be grouped into two categories, according to their structural homologies. dPak is homologous to type 1 Paks, which is known to form inactive dimmers via the N-terminal autoinhibitory (AI) domain. When type 1 Paks are activated by Cdc42 and Rac, this binding would rearrange local conformations of the AI domain, releasing the activation loop and dissociating the dimer. Considering the drastic conformational change after activation, we wonder if Henji has any preference to target

only certain form(s) of dPak. Three forms of UAS-dPak transgenes are generated by T. T. Lai according to the structure-based studies. The constitutive active form of dPak contains a point-mutation of T423E, mimicking a constitutively phosphorylation at the first autophosphorylation site. Expression of T423E Pak CA construct is sufficient to promote motility, and anchorage-independent growth via the MAPK kinase pathway in human breast cancer lines (Vadlamudi *et al*., 2000). On the other hand, the dominant negative form of dPak carries three point-mutation, H83L/H86L/K299R, with the former two mutations disrupting the interaction with Cdc42/Rac1 and the later being a kinase dead mutation. This construct is also proved to inhibit the downstream activation of Ras signaling in mammalian cell lines (Tang *et al.*, 1997). The last construct is made from full-length wildtype dPak. The expression of these constructs is tested by immunoblotting using specific anti-Myc antibody (Figure 3A). Both Myc-tagged dPak CA and dPak DN are successfully overexpressed in muscle cells using C57-GAL4; however, Myc-dPak wt lines are somewhat problematic. The UAS-Myc-dPak wt construct is not defective in its construct sequence. More lines will be generated in order to obtain strong, proper-expressing ones.

Myc-dPak CA and dPak DN constructs are overexpressed postsynaptically with muscle-specific C57-GAL4 and then GluRIIA intensity is analyzed as a terminal phenotype in response to dPak activity at the synapse. However, the abundance of

GluRIIA in all three forms of dPak overexpression is similar to *C57-GAL4, henji*$^{+/-}$ heterozygous control (Figure 3B-E), while *C57-GAL4, henji*^{2}*/henji*^{1} mutant still shows an enhanced GluRIIA clustering (Figure3G). Nevertheless, this data is consistent with the previous report that overexpressing myristoylated dPak, mimicking a constitutively active form, in wildtype flies is not sufficient to upregulate GluRIIA abundance at *Drosophila* NMJs (Albin and Davis, 2004).

In our hypothesis, Henji is responsible to specifically downregulate dPak at the NMJs. When dPak CA is overexpressed postsynaptically, Henji rapidly promotes the degradation of the excess dPak protein. Therefore, even though it is the CA form of dPak overexpressed, the functional dPak protein at the synapse is not sufficient to promote additional GluRIIA clustering to the PSDs. In order to prove this hypothesis, these three dPak constructs are overexpressed with C57-GAL4 in *henji*$^{+/-}$ flies. Strikingly, GluRIIA punctae intensity is further enhanced in dPak CA overexpressing flies compared with *C57-GAL4, henji*$^{+/-}$ heterozygous control and even stronger than *C57-GAL4, henji*^{2}*/henji*^{1}mutant (Figure 3F-H). On the other hand, GluRIIA clustering is significantly inhibited in dPak DN overexpressing *henji*$^{+/-}$ NMJs (Figure3F,G and I). To know whether the overexpressed dPak is localized to the synapse and thus perform its function to enhance GluRIIA clustering, anti-Myc antibody (9E10) is employed for staining. When Myc-dPak CA or dPak DN is overexpressed in the muscle, the overall

background signal of Myc staining is elevated in the muscle cell compared with *C57-GAL4* control (Figure 3J, K and M). However, when these constructs are overexpressed in *henji*$^{+/-}$ flies, strong Myc-positive punctae appear and specifically surround the NMJ (Figure 3L and N). These results indicate a role for Henji to very specifically regulate local dPak protein levels at the PSDs and this regulation is not related to the active states of dPak.

Chapter 5. Discussion

5-1. Bifurcated signaling downstream of βν/FAK56

Ras/MAPK signaling was shown to specifically downregulate FasII level at the synapse and this negative regulation is well-correlated to bouton addition (Koh et al., 2002). On the other hand, PKA was shown to affect transmitter release from the presynapse (Davis et al., 1998); mutants defects in cAMP production also showed abnormal bouton growth (Cheung et al., 1999). In both cases, the upstream cue modulates activities of Ras or cAMP was not clearly defined. In this study, we described an integrin βν-mediated ECM signaling, distinct form BMP/Gbb or Wnt/Wg pathways, functions to restrain NMJ bouton growth. This pathway included the activation of FAK56 and further elevation of cAMP signal by NF1 and inhibiton of Ras/MAPK via Vap. These two bifurcated signaling pathways finally converge to regulate synaptic growth.

5-2. Cullin3/Henji E3 complex affects postsynaptic GluRIIA/GluRIIB ratio by downregulating dPak protein level

During the development of the NMJ, strengthening of both neurotransmission and synaptic structure requires modulations in local protein level and proper localization. When GluRIIA expression is augmented in the postsynapse by either UAS-GluRIIA

transgene overexpression or genetically reduce *glurIIB* gene dosage, proper clustering of IIA-containing GluRs were formed at PSDs and the evoked response and synaptic bouton number were significantly elevated (Sigrist et al., 2002). In our experiments, we have identified a Cullin 3-based E3 ligase comples responsible for regulating the GluR subunit composition at the postsynapse. In *henji* mutant, the GluRIIA/GluRIIB ratio is increased and this alteration corresponded to the enhanced muscle response to the presynaptic spontaneous vesicle release.

The postsynaptic GluRIIA localization requires dPak activity but when constitutively active, membrane-bound dPak transgene was overexpressed postsynaptically, GluRIIA abundance was not further enhanced (Albin et al., 2004). We generated a constitutively phosphorylated dPak transgene and consistently, overexpression of this dPak CA in the muscle did not change GluRIIA. However, when this construct was postsynaptically overexpressed in *henji*$^{+/-}$ background, GluRIIA clustering at PSDs were dramatically enhanced. Therefore, we propose that Henji is required at the synapse to regulate dPak protein level and further influence local GluRIIA abundance; GluRIIA CA construct expressed in wildtype synapse, this protein would be rapidly downregulated by Henji and thus had no effects on GluRIIA abundance.

5-3. Neuortransmission homeostasis is not disrupted in henji mutant

Brp-positive punctae were quantified and in henji mutant there was a 20% increase in total release sites per NMJ (Appendix 5B). However, EJP remained unaltered in henji mutant regardless to the increase of both release sites and boutons, showing intact homeostatic machinery. The enhanced postsynaptic GluRIIA augments muscle response to neurotransmitter released; to compensate such hyper-sensitivity of the postsynapse and to maintain synaptic homeostasis in neurotransmission, presynaptic vesicle release machinery was attenuated to keep EJP unchanged. The enhanced synaptic structure and expanded AZs were suppressed by this homeostatic compensation.

Materials and methods

Fly stocks

All flies were reared in standard conditions at 25℃. We use w^{1118} from Bloomington stock center as wild-type in this study. Mutant flies *integrin*βv^{1} and βv^{2} have been described previously (Devenport and Brown, 2004). *N30* and *K24* deletions of *FAK56* were generated from *KG00304* P-element insertion as previously described as Tsai et al., 2008. The transgenic lines elav-GAL4 (X) and elav-GAL4 (III) were obtained from the Bloomington stock center. MHC-GAL4. vap^{1} and vap^{2} mutant flies were kind gifts from Dr. S. Schneuwly's lab and the alleles were as described (Botella et al., 2003). $NF1^{E2}$, *w; iso2;iso3, hs-NF1 wt, hs-NF1 KA, hs-NF1 RP, UAS-NF1 GRD, UAS-NF1 GRD KA, UAS-NF1 GRD RP and UAS-NF1* Δ*GRD* transgenic flies were generated by Dr. J. Walker. The nature of NF1-related mutant alleles were as previously described (Walker et al., 2006).

Immunostaining

Wandering third instar larvae were dissected for analysis of NMJ phenotypes in all experiments. Dissected larval fillets were incubated in fixative solution (4% formaldehyde in 1× phosphate-buffered saline) for 20 minutes. The following primary antibodies were used for immunostainig: anti-synaptotagmin (mouse, 1:25; DSHB),

anti-synapsin (3C11, 1:100; DSHB), HRP conjugated with TRITC (rabbit, 1:100; Jackson ImmunoResearch), anti-FasII (1D4, 1:100; DSHB), anti-Brp (Nc82, 1:100; DSHB), anti-Dlg (mouse, 1:100; DSHB), anti-dGluRIIA (mouse, 1:100; DSHB), anti-Futsch (22C10, 1:100; DSHB) and anti-GFP (chicken, 1:1000; Abcam). Alexa 488-, FITC-, TRITC-, Cy3- and Cy5-conjugated secondary antibodies and FITC-phalloidin were used (Jackson ImmunoResearch).

Image processing and presentation

Confocal images were acquired using Zeiss LSM 510 Meta or Zeiss LSM 710. Images were processed using Adobe Photoshop CS. Bouton number and muscle area were quantified with Zeiss LSM 510 image examination software. For comparison and quantification of signal intensity at NMJs, larval fillets were stained in the same tube and the images were acquired under the same scanning parameters. NMJ silhouettes were outlined and the signal intensity was calculated by histogram analysis using Adobe Photoshop CS.

Transgenes

UAS-βv-GFP was made by cloning the full-length *βv* insert from cDNA library into pTWG vector (DGRC) using the Gateway recombination cloning system (Invitrogen). The resulting construct carries a C-terminal GFP tag. *UAS-GFP-vap* wt and *UAS-GFP-vap R695K* were cloned from cDNA library; Missense point mutation of R695K was made by PCR-based mutagenesis. Both inserts were cloned into pTGW vector from DGRC and the Gateway recombination cloning system was also used. All constructs were checked by sequencing prior to embryo microinjection. Transgenic flies were generated by standard procedures.

Electrophysiological recording

For sample preparation, dissected larval body walls (including the central nervous system and motor axons) were exposed in cold (4°C) HL3.1 Ca2+ free saline (70 mM NaCl, 5 mM KCl, 4 M MgCl2, 10 mM NaHCO3, 5 mM trehalose, 115 mM sucrose, 5 mM HEPES pH 7.2) [66]. Experiments were performed on muscle 6 of segment A3 in late third instar larvae. The segmental nerve was cut near the ventral ganglion. Preparations were then incubated in HL3.1 saline containing 0.2 or 1 mM CaCl2 for electrophysiological experiments at room temperature (22°C). For stimulation and recording, a glass microelectrode (30–50 MO in resistance) filled with 3 M KCl was

impaled in the sixth muscle of the third abdominal segment to record the EJPs. The mEJPs occurring in the background within 200 seconds were obtained without any stimulation on the segmental nerve. To evoke an EJP, the segmental nerve was stimulated every 30 seconds through the cut end with a suction electrode with 0.1 ms of pulse duration at 2 times the threshold voltage. Once the threshold voltage was reached, the size of EJPs remained unchanged despite the increase in stimulating voltage. Signals were digitized at 64 KHz by a PCI-6221 data acquisition card (National Instrument, Austin, Texas, USA), and saved on an IBM compatible PC for analysis.

Western blots

Third instar larvae or adult heads of different genotypes were homogenized in in RIPA lysis buffer. Equal amounts of lysates were separated in 7.5% or 8% SDS-PAGE gel. Blots were probed with anti-dPak (rabbit, 1:10,000), anti-Myc (9E10, 1:1000, Santa Curz), anti-GFP (mouse, 1:1000, Invitrogen), anti-a tubulin (mouse, 1:200,000, Sigma) and HRP conjugated secondary antibodies.

Dibutyl cAMP/forskolin feeding

Adult $NF1^{E2}$ flies were put into vials containing standard medium mixed with 10nM of di-cAMP or forskolin. After 6 hours all adult flies were transferred into another vial

filled with standard medium and the eggs laid on media mixed with di-cAMP or forskolin were reared until late third instar when they were dissected and NMJ morphology analyzed.

Electron Microscopy

For ultrastructural NMJ studies larval fillets were dissected at room temperature in calcium free medium and subsequently fixed overnight in 4% paraformaldehyde /1% glutaraldehyde/0.1 M cacodylic acid (pH 7.2). Microwave irradiation (MWI) with the PELCO BioWave® 34700 laboratory microwave system was used for subsequent EM processing steps. After overnight fixation, the fixed fillets were additionally post-fixed with 1% aqueous osmium tetroxide 2x at 90W for 2minON-2minOFF-2minON under vacuum and placed on ice in between changes with additional 1 hour incubation on rotator, dehydrated in increasing ethanol concentrations(50%,70%,80%,90%,100%) 1x at 150W for 40s each,. Samples were gradually infiltrated with increasing resin to propylene oxide ratio up to full resin 2x at 250W for 3min each under vacuum. The samples were embedded in flat silicone mold with EMBED-812 resin and cured in the oven at 60℃

References

Albin, S. D. and G. W. Davis (2004). "Coordinating structural and functional synapse development: postsynaptic p21-activated kinase independently specifies glutamate receptor abundance and postsynaptic morphology." J Neurosci 24(31): 6871-6879.

Beumer, K. J., J. Rohrbough, et al. (1999). "A role for PS integrins in morphological growth and synaptic function at the postembryonic neuromuscular junction of Drosophila." Development 126(24): 5833-5846.

Chan, C. S., E. J. Weeber, et al. (2003). "Integrin requirement for hippocampal synaptic plasticity and spatial memory." J Neurosci 23(18): 7107-7116.

Chan, C. S., E. J. Weeber, et al. (2006). "Beta 1-integrins are required for hippocampal AMPA receptor-dependent synaptic transmission, synaptic plasticity, and working memory." J Neurosci 26(1): 223-232.

Ciechanover, A. and P. Brundin (2003). "The ubiquitin proteasome system in neurodegenerative diseases: sometimes the chicken, sometimes the egg." Neuron 40(2): 427-446.

Collins, C. A. and A. DiAntonio (2007). "Synaptic development: insights from Drosophila." Curr Opin Neurobiol 17(1): 35-42.

Deshaies, R. J. (1999). "SCF and Cullin/Ring H2-based ubiquitin ligases." Annu Rev

Cell Dev Biol 15: 435-467.

DiAntonio, A. (2006). "Glutamate receptors at the Drosophila neuromuscular junction." Int Rev Neurobiol 75: 165-179.

DiAntonio, A., S. A. Petersen, et al. (1999). "Glutamate receptor expression regulates quantal size and quantal content at the Drosophila neuromuscular junction." J Neurosci 19(8): 3023-3032.

Dickman, D. K., Z. Lu, et al. (2006). "Altered synaptic development and active zone spacing in endocytosis mutants." Curr Biol 16(6): 591-598.

Featherstone, D. E. and K. Broadie (2000). "Surprises from Drosophila: genetic mechanisms of synaptic development and plasticity." Brain Res Bull **53**(5): 501-511.

Furukawa, M., Y. J. He, et al. (2003). "Targeting of protein ubiquitination by BTB-Cullin 3-Roc1 ubiquitin ligases." Nat Cell Biol **5**(11): 1001-1007.

Geiger, B., A. Bershadsky, et al. (2001). "Transmembrane crosstalk between the extracellular matrix--cytoskeleton crosstalk." Nat Rev Mol Cell Biol 2(11): 793-805.

Geyer, R., S. Wee, et al. (2003). "BTB/POZ domain proteins are putative substrate adaptors for cullin 3 ubiquitin ligases." Mol Cell **12**(3): 783-790.

Gramates, L. S. and V. Budnik (1999). "Assembly and maturation of the Drosophila larval neuromuscular junction." Int Rev Neurobiol 43: 93-117.

Hing, H., J. Xiao, et al. (1999). "Pak functions downstream of Dock to regulate

photoreceptor axon guidance in Drosophila." Cell **97**(7): 853-863.

Keshishian, H., K. Broadie, et al. (1996). "The drosophila neuromuscular junction: a model system for studying synaptic development and function." Annu Rev Neurosci **19**: 545-575.

Khuong, T. M., R. L. Habets, et al. (2010). "WASP is activated by phosphatidylinositol-4,5-bisphosphate to restrict synapse growth in a pathway parallel to bone morphogenetic protein signaling." Proc Natl Acad Sci U S A 107(40): 17379-17384.

Marrus, S. B., S. L. Portman, et al. (2004). "Differential localization of glutamate receptor subunits at the Drosophila neuromuscular junction." J Neurosci **24**(6): 1406-1415.

Nelson, P. G., M. A. Lanuza, et al. (2003). "Phosphorylation reactions in activity-dependent synapse modification at the neuromuscular junction during development." J Neurocytol **32**(5-8): 803-816.

Qin, G., T. Schwarz, et al. (2005). "Four different subunits are essential for expressing the synaptic glutamate receptor at neuromuscular junctions of Drosophila." J Neurosci **25**(12): 3209-3218.

Rasse, T. M., W. Fouquet, et al. (2005). "Glutamate receptor dynamics organizing synapse formation in vivo." Nat Neurosci **8**(7): 898-905.

Rohrbough, J., M. S. Grotewiel, et al. (2000). "Integrin-mediated regulation of synaptic morphology, transmission, and plasticity." J Neurosci 20(18): 6868-6878.

Ruiz-Canada, C. and V. Budnik (2006). "Synaptic cytoskeleton at the neuromuscular junction." Int Rev Neurobiol 75: 217-236.

Schmid, A., S. Hallermann, et al. (2008). "Activity-dependent site-specific changes of glutamate receptor composition in vivo." Nat Neurosci **11**(6): 659-666.

Schuster, C. M., G. W. Davis, et al. (1996). "Genetic dissection of structural and functional components of synaptic plasticity. II. Fasciclin II controls presynaptic structural plasticity." Neuron 17(4): 655-667.

Sigrist, S. J., P. R. Thiel, et al. (2002). "The postsynaptic glutamate receptor subunit DGluR-IIA mediates long-term plasticity in Drosophila." J Neurosci **22**(17): 7362-7372.

Sone, M., E. Suzuki, et al. (2000). "Synaptic development is controlled in the periactive zones of Drosophila synapses." Development **127**(19): 4157-4168.

Tang, Y., Z. Chen, et al. (1997). "Kinase-deficient Pak1 mutants inhibit Ras transformation of Rat-1 fibroblasts." Mol Cell Biol **17**(8): 4454-4464.

Torroja, L., M. Packard, et al. (1999). "The Drosophila beta-amyloid precursor protein homolog promotes synapse differentiation at the neuromuscular junction." J Neurosci **19**(18): 7793-7803.

Tsai, P. I., H. H. Kao, et al. (2008). "Fak56 functions downstream of integrin

alphaPS3betanu and suppresses MAPK activation in neuromuscular junction growth." Neural Dev 3: 26.

Vadlamudi, R. K., L. Adam, et al. (2000). "Regulatable expression of p21-activated kinase-1 promotes anchorage-independent growth and abnormal organization of mitotic spindles in human epithelial breast cancer cells." J Biol Chem **275**(46): 36238-36244.

Yi, J. J. and M. D. Ehlers (2005). "Ubiquitin and protein turnover in synapse function." Neuron **47**(5): 629-632.

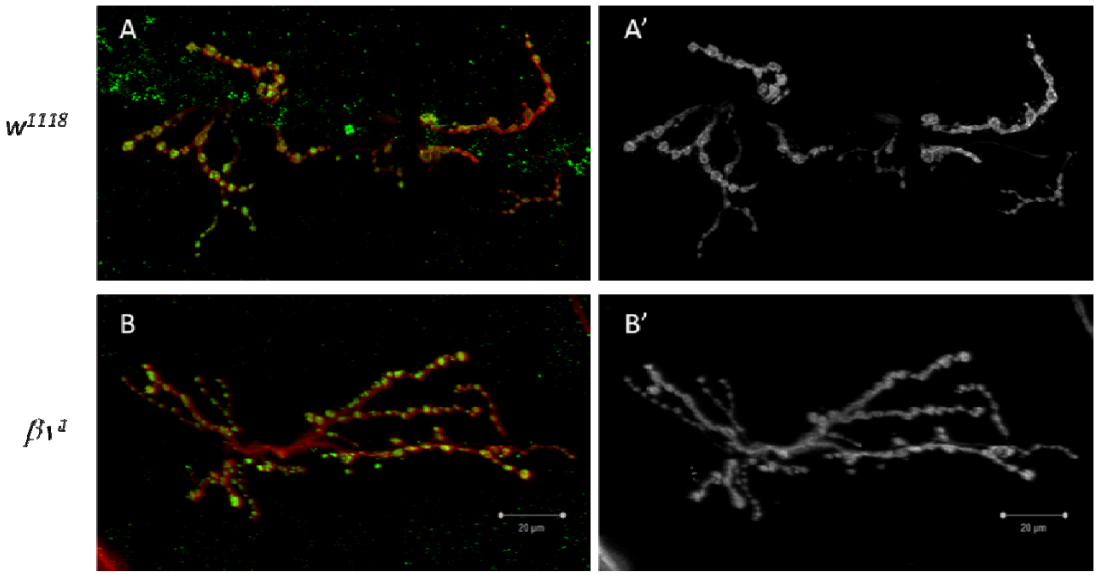
A
A′
B
B′
w1118
β1d
20 μm
20 μm

C

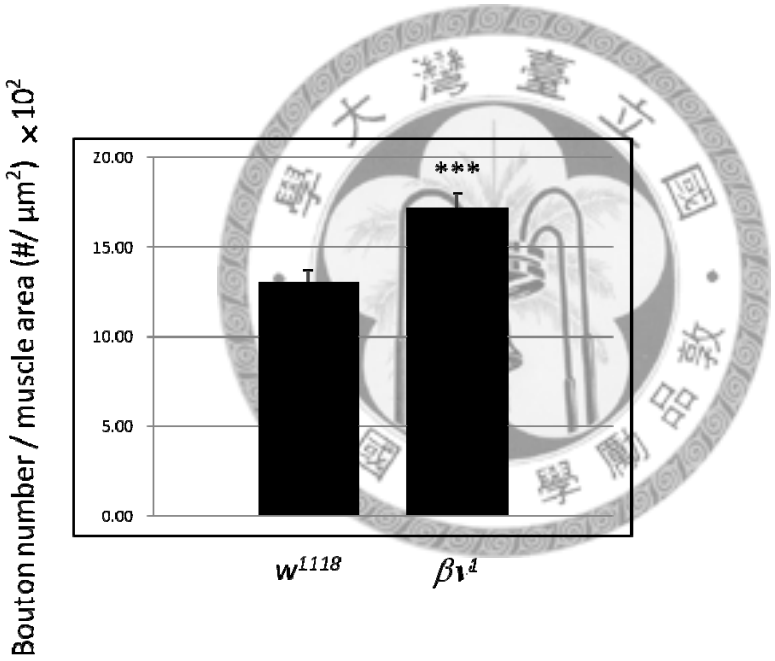
Bouton number / muscle area (#/ μm2) x 10-2
20.00
15.00
10.00
5.00
0.00
***
w1118
β1d

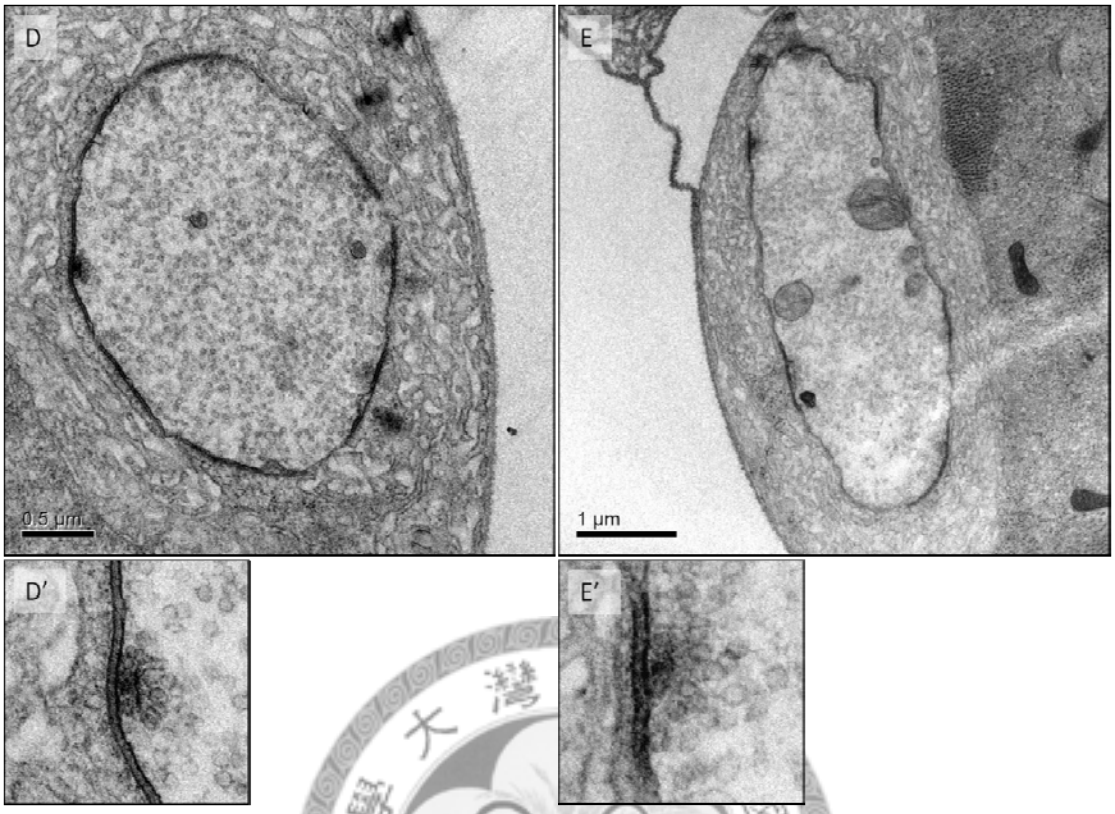

Figure 1. $\beta\nu$ mutant displays overgrowth NMJ phenotype.

(A) (B) Third instar larvae were dissected and co-immunostained with HRP and Syn. NMJ6/7 from A3 segment were photographed. $\beta\nu^{1}$ mutant has overgrown NMJ phenotype (B) as compared to wildtype (A). (C) Bouton number is significantly increased in $\beta\nu^{1}$ mutant. Triple-asterisks indicate significance by Student's t test ($p < 0.001$) and error bars represent the standard error of the mean (SEM). (D)(E) Electron micrographic sections of type I bouton in $\beta\nu^{1}$/+ heterozygous control (D) and $\beta\nu^{1}$ larvae (E). Lower panels show electron-densed active zones with a clear T bar. Though sample number is not large enough for meaningful quantification, no significant alterations in SSR morphology, bouton size, active zone length, vesicle size and number, T-bar morphology and number are observed.

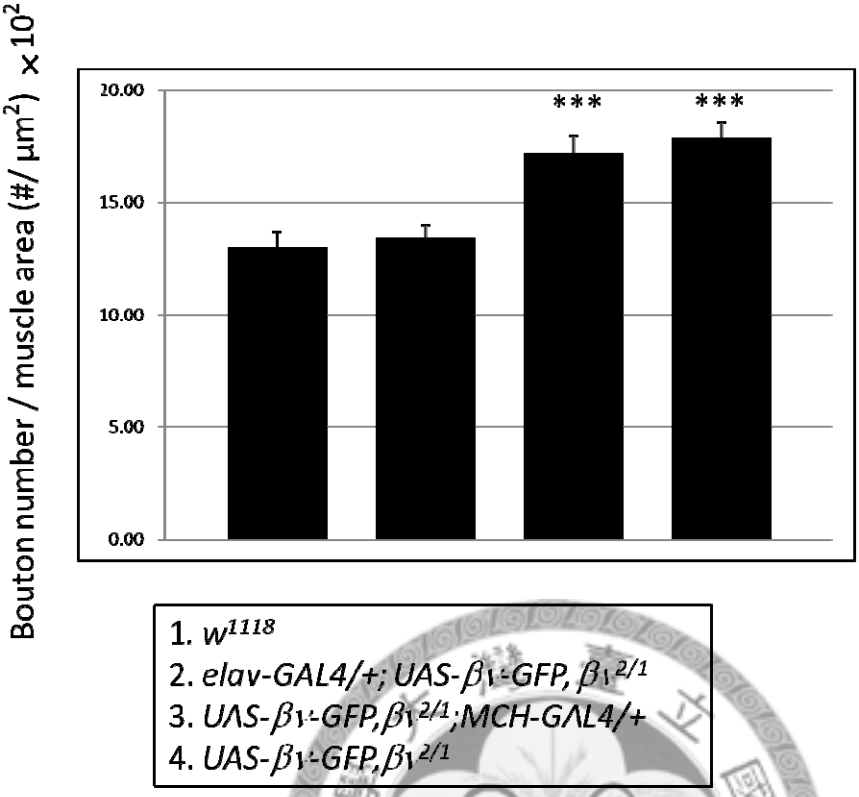

Figure 2. *βν* is required presynaptically to regulate bouton growth.

The same UAS-βν-GFP line is used in this experiment to compare the expression level of this transgene. Bar 3 and bar 4 differ statistically significant from w^{1118} control shown by bar 1 (both $p < 0.001$). *elav>βν-GFP* rescued the bouton-overaddition phenotype in $\beta\nu^{1/2}$ mutant and their bouton number is not significantly different from wildtype control ($p > 0.05$).

A

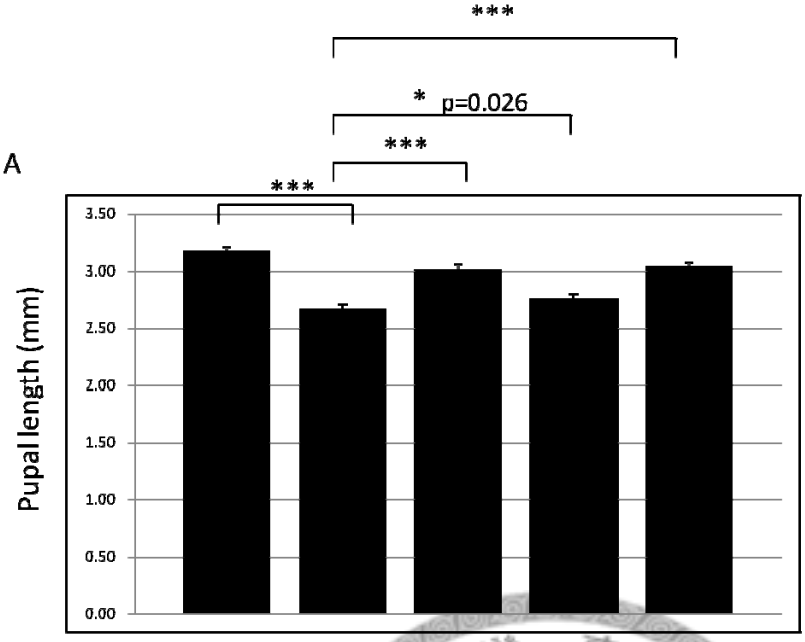

1. *iso2; iso3*
2. *NF1^{E2}*
3. *elav-GAL4; UAS-NF1 GRDwt; NF1^{E2}*
4. *elav-GAL4; UAS-NF1 GRDRP; NF1^{E2}*
5. *elav-GAL4; UAS-NF1-GRDwt*

B

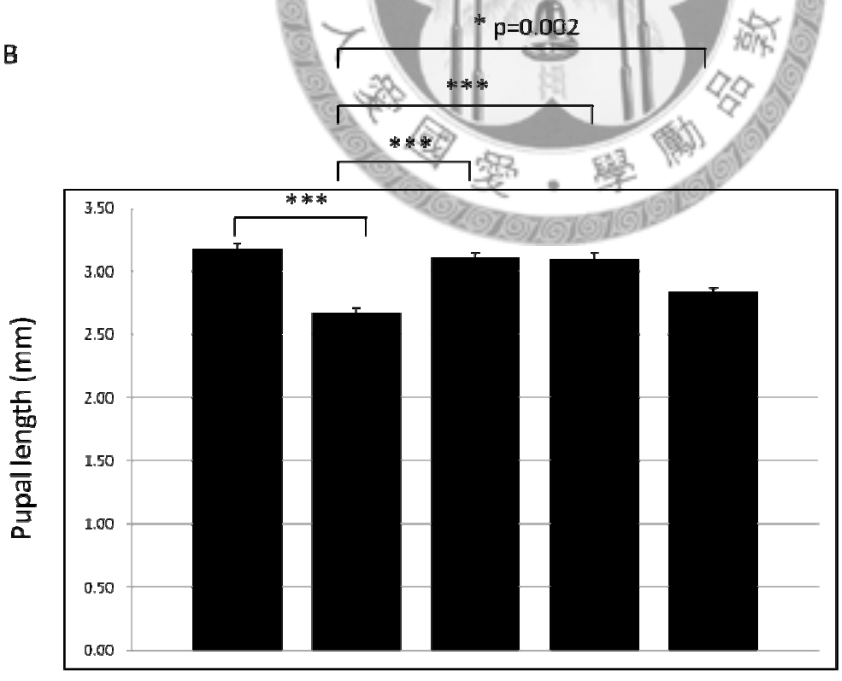

1. *iso2; iso3*
2. *NF1^{E2}*
3. *hs-NF1 wt; NF1^{E2}*
4. *hs-NF1 KA; NF1^{E2}*
5. *hs-NF1 ΔGRD, NF1^{E2}*

Figure 3. GRD of NF1 is both required and sufficient to rescue reduced *NF1* mutant body length.

(A) Isogenic fly *iso2; iso3* were used to generate the $NF1^{E2}$ null mutant; therefore this line was used as a control. Pupal length was measured with a caliper gauge with resolution for 0.01mm. Triple-asterisks indicate significance by Student's t test ($p < 0.001$). Asterisk represents significance with $p < 0.05$. (B) All the flies, including *iso2;iso3* control and $NF1^{E2}$ were put into the same heat-shock procedure at the same time. Embryos of 24hours AEL (after egg-laying) were heat-shocked in 37℃ water bath for 30 minutes. This transient heat-shock was repeated every 24 hours until late pupal stage. Then the pupal were picked out and their lengths measured under a dissecting microscope.

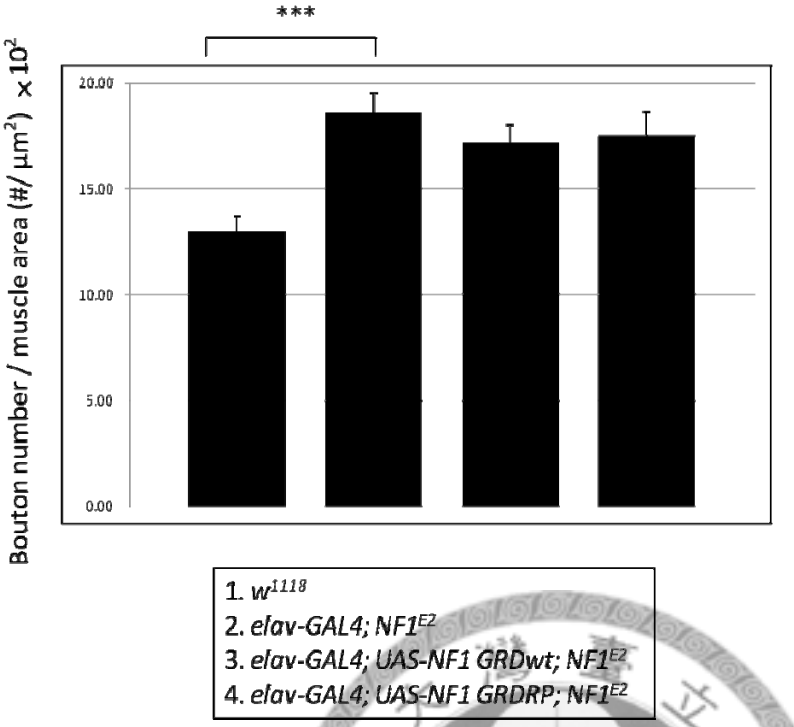

Figure 4. GRD of NF1 is not essential for the regulation of bouton addition.

Neuronal expression of wildtype NF1 GRD failed to rescue $NF1^{E2}$ NMJ overgrowth phenotype (p=0.26). Similarly, NF1 GRD RP also failed to restore $NF1^{E2}$ NMJ.

A

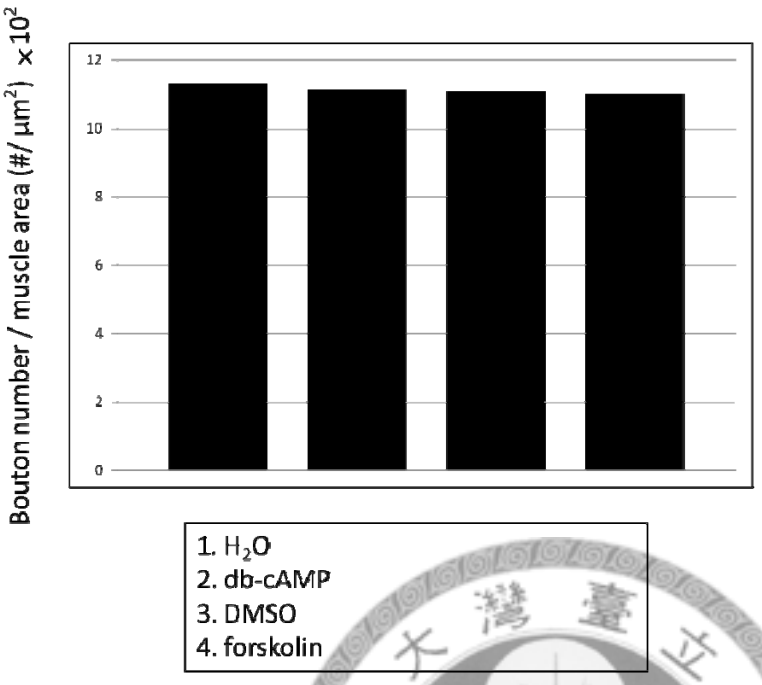
Bouton number / muscle area (#/ μm²) ×10²
12
10
8
6
4
2
0
1. H2O
2. db-cAMP
3. DMSO
4. forskolin

B

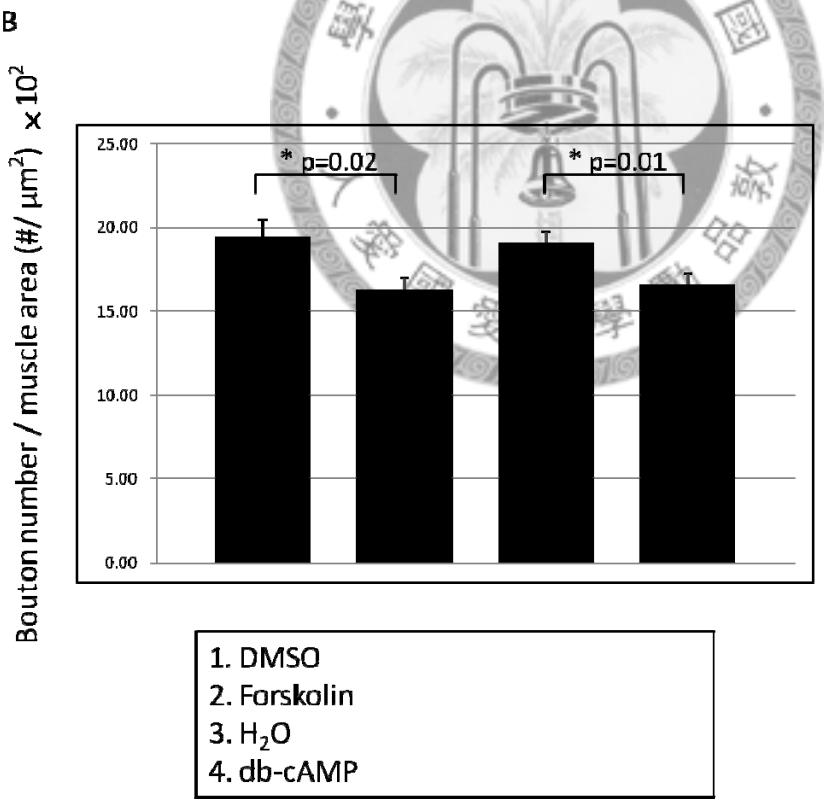
Bouton number / muscle area (#/ μm²) ×10²
25.00
20.00
15.00
10.00
5.00
0.00
* p=0.02
* p=0.01
1. DMSO
2. Forskolin
3. H2O
4. db-cAMP

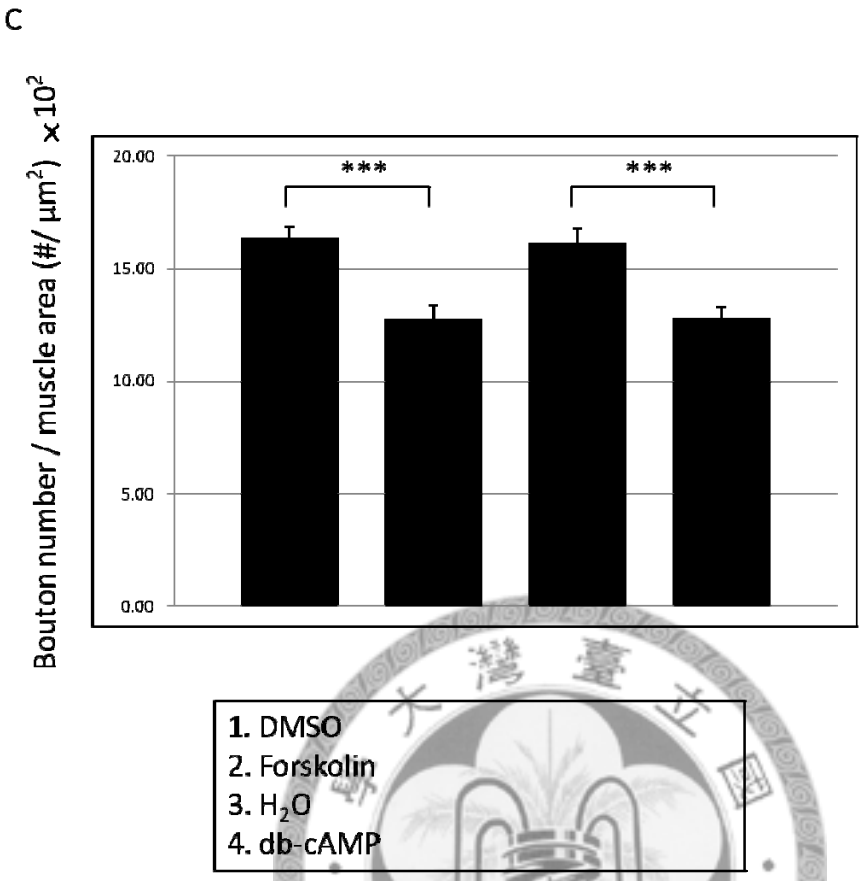

Figure 5. βν and NF1 regulates bouton number through cAMP-dependent pathway.

(A) w^{1118} wildtype larvae were reared in food containing DMSO, forskolin, distilled water or dibytyl cAMP (di-cAMP). Bouton numbers of wandering third instar larvae were counted and normalized to muscle 6/7 areas. $\beta\nu^{J}$ mutant larvae (B) and $NF1^{E2}$ null mutant larvae (C) fed with the same chemicals as in (A).

A

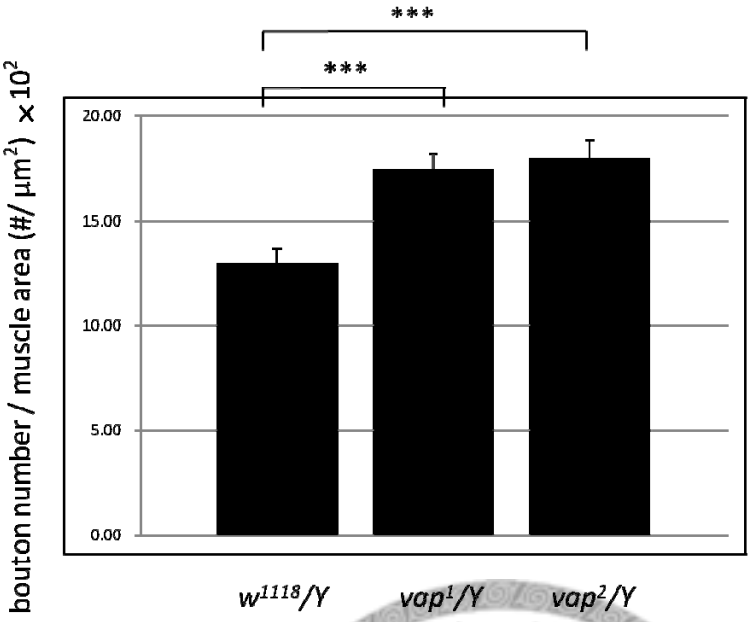

B

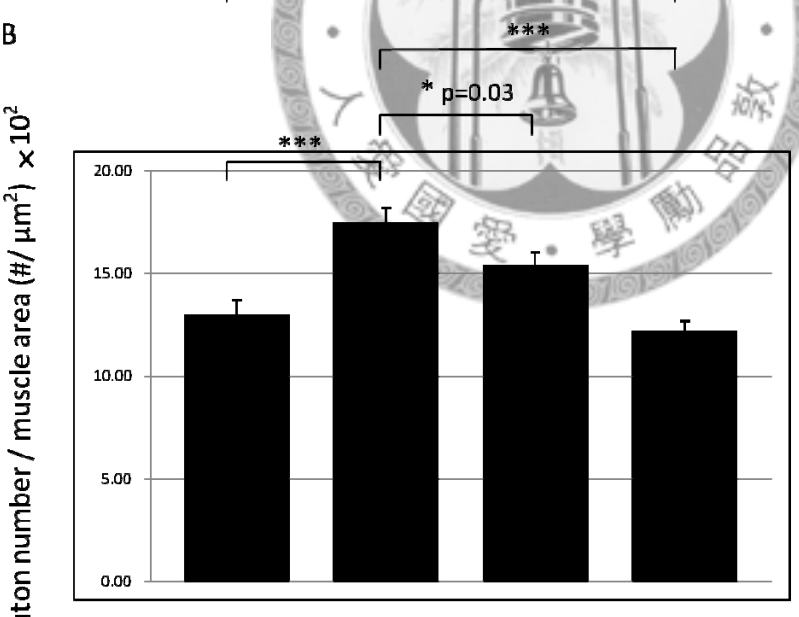

1. $w^{1118/Y}$
2. vap^{1}/Y
3. vap^{1}/Y; UAS-RasGAP/+; OK319-GAL4/+
4. vap^{1}/Y; UAS-RasGAP/+; elav-GAL4/+

Figure 6. Vap is required in the presynapse to regulate bouton addition.

(A) Bouton numbers from two vap mutants were compared with wildtype. Only male larvae from both *vap*^{1} and *vap*^{2} mutants have overgrown NMJ phenotype. Female larvae of *vap*^{1} mutant show bouton number comparable to wildtype NMJs. n.s. stands for non-significant by Student's t-test. (B) Vap is required in the presynapse to regulate bouton addition. Presynaptic expression of *UAS-RasGAP* transgene with *OK319-GAL4* partially rescued the overgrown NMJs in *vap*^{1}. On the other hand, *elav-GAL4* driven neuronal expression of the same transgene rescued excess boutons found in *vap*^{1}.

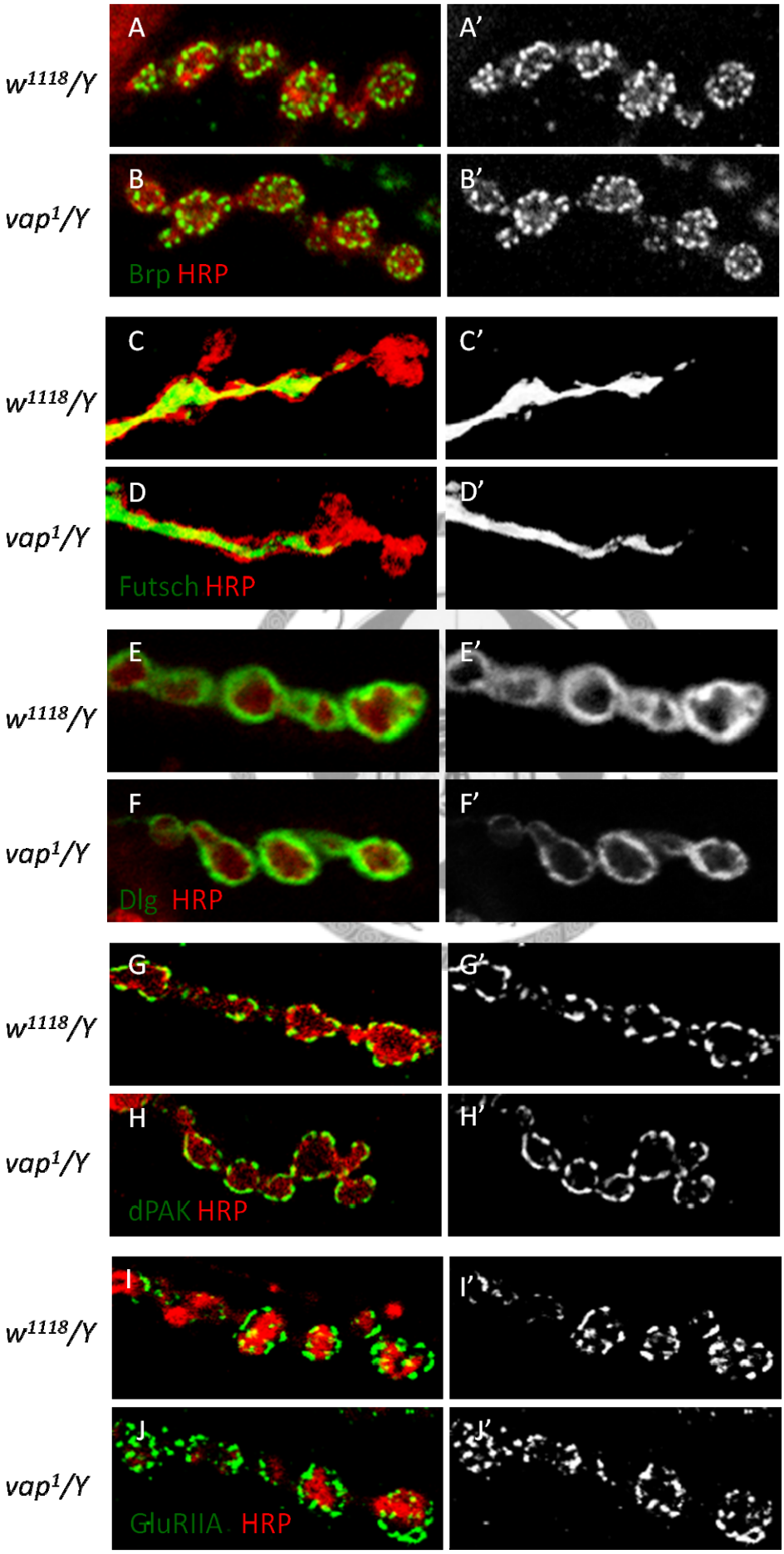
w1118/Y
A
A'
vap1/Y
B
B'
Brp HRP
w1118/Y
C
C'
vap1/Y
D
D'
Futsch HRP
w1118/Y
E
E'
vap1/Y
F
F'
Dlg HRP
w1118/Y
G
G'
vap1/Y
H
H'
dPAK HRP
w1118/Y
I
I'
vap1/Y
J
J'
GluRIIA HRP

Figure 7. Synaptic marker staining in vap mutant.

(A-J) Expression pattern of Brp at presynaptic active zones (green in (A) and (B), white in (A') and (B')), Futsch for presynaptic microtubule structure (green in (C) and (D), white in (C') and (D')), Dlg in postsynapse (green in (E) and (F), white in (E') and (F')), dPak (green in (G) and (H), white in (G') and (H')) and GluRIIA (green in (I) and (J), white in (I') and (J')) at PSDs. All images were acquired form confol sigle sections; only Futsch images come from Z-stack projection of all single sections. For GluRIIA staining, Bouin's fixative soulution (Sigma) was used. Staining for other markers were under standard procedure.

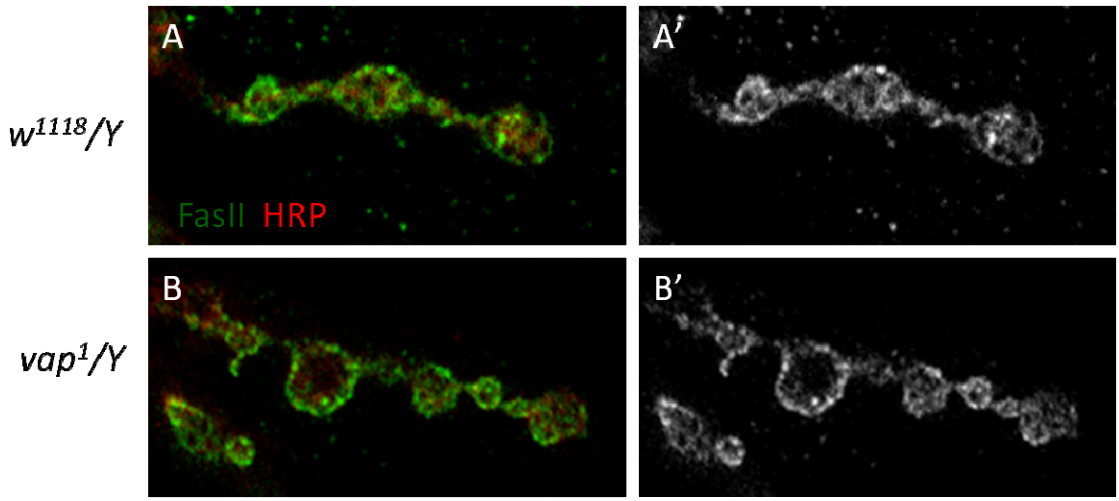

Figure 8. FasII intensity at the NMJ is reduced in *vap* mutant.

(A) (B) Expression of FasII (green in (A) and (B), white in (A') and (B')) at NMJ 6/7 in wildtype (A) and male vap1 mutant (B). HRP was co-stained and shown in red. Images were confocal single sections. (C) Quantification of FasII intensity relative to HRP immunoreactivity of the same area. *vap*^{1} mutant showed reduced FasII level in the peri-active zone. Triple-asterisks indicate significant difference by Student's t test ($p < 0.05$) and error bars represent the standard error of the mean (SEM).

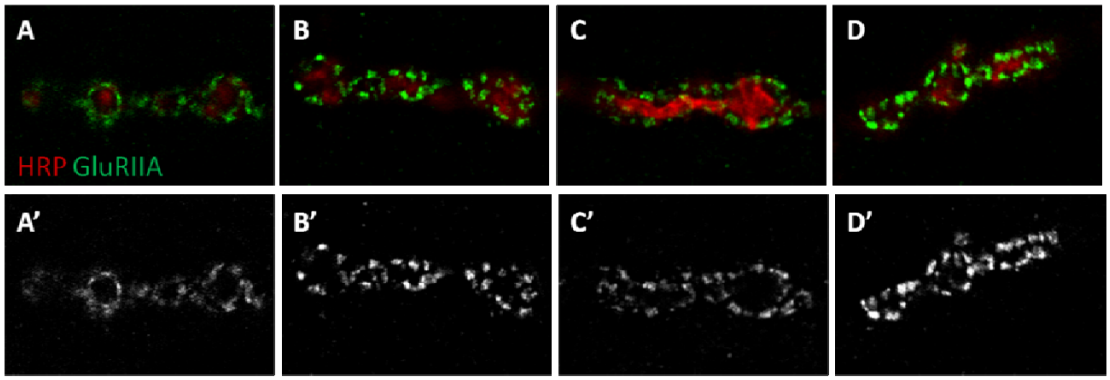

A. *henji*^{1}/+
B. *henji*$^{1/2}$
C. *UAS-henji; C57-GAL4, henji*^{2}/*henji*^{1}
D. *elav-GAL4; UAS-henji; henji*^{1}

E

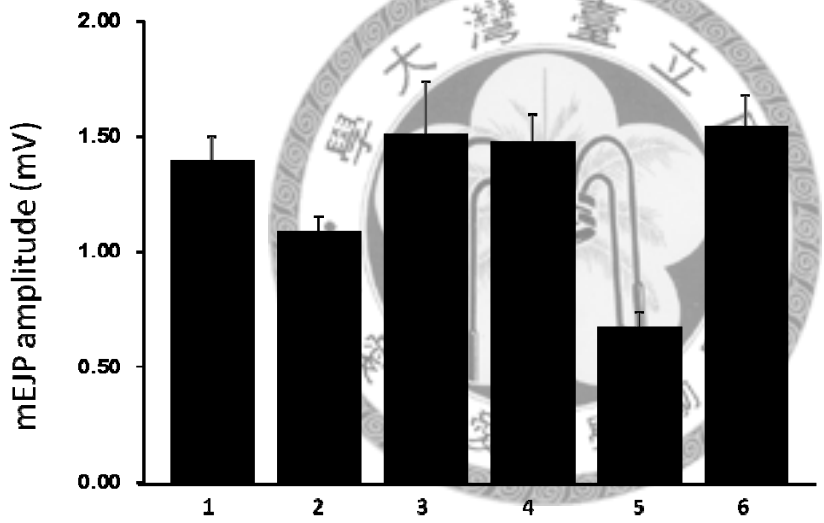

1. *w*^{1118}
2. *C57-GAL4; henji*^{2}/+
3. *ELAV-GAL4; henji*^{2}/+
4. *C57-GAL4; henji*^{1}/*henji*^{2}
5. *UAS-henji; C57-GAL4, henji*^{2}/+
6. *elav-GAL4; UAS-henji; henji*^{2}/+

Figure 9. Postsynaptic overexpression of Henji rescues GluRIIA abundance and mEJP amplitude increase in *henji* mutant. (A-D) NMJs at muscle 4 of wandering third instar larvae are labeled with anti-HRP and anti-dGluRIIA. Lower panel, only GluRIIA signals are shown. The intensity of GluRIIA punctae is elevated in *henji* mutant but restored to wildtype level when Henji is expressed in the muscle cell. (E) mEJP amplitude. Error bars represent S.E.M.

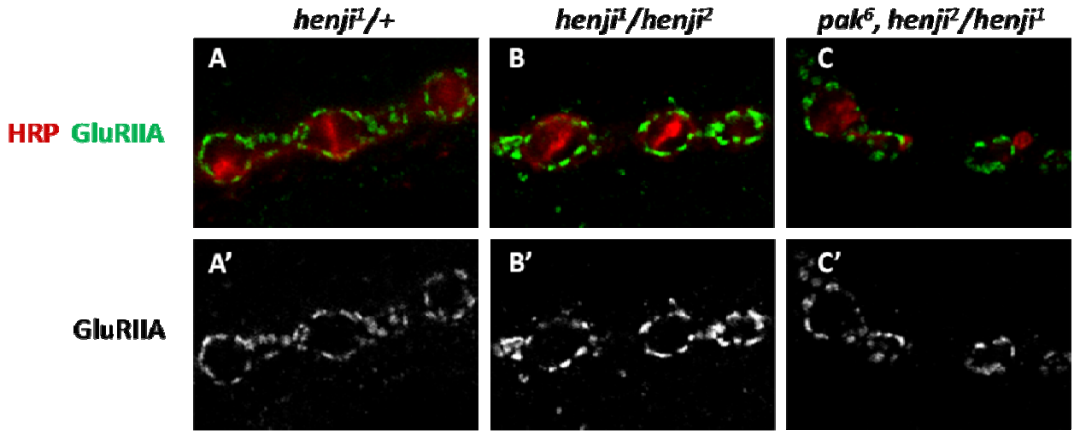

Figure 10. Loss of one copy of *dpak* restores postsynaptic GluRIIA clustering. (A-C) NMJ4 from larval body wall muscle A2-A6 is labeled with anti-HRP and anti-dGluRIIA. Introduction of *pak6* null allele reduces *pak* gene copies and suppresses the enhancement of GluRIIA intensity in *henji*$^{1/2}$ mutant.

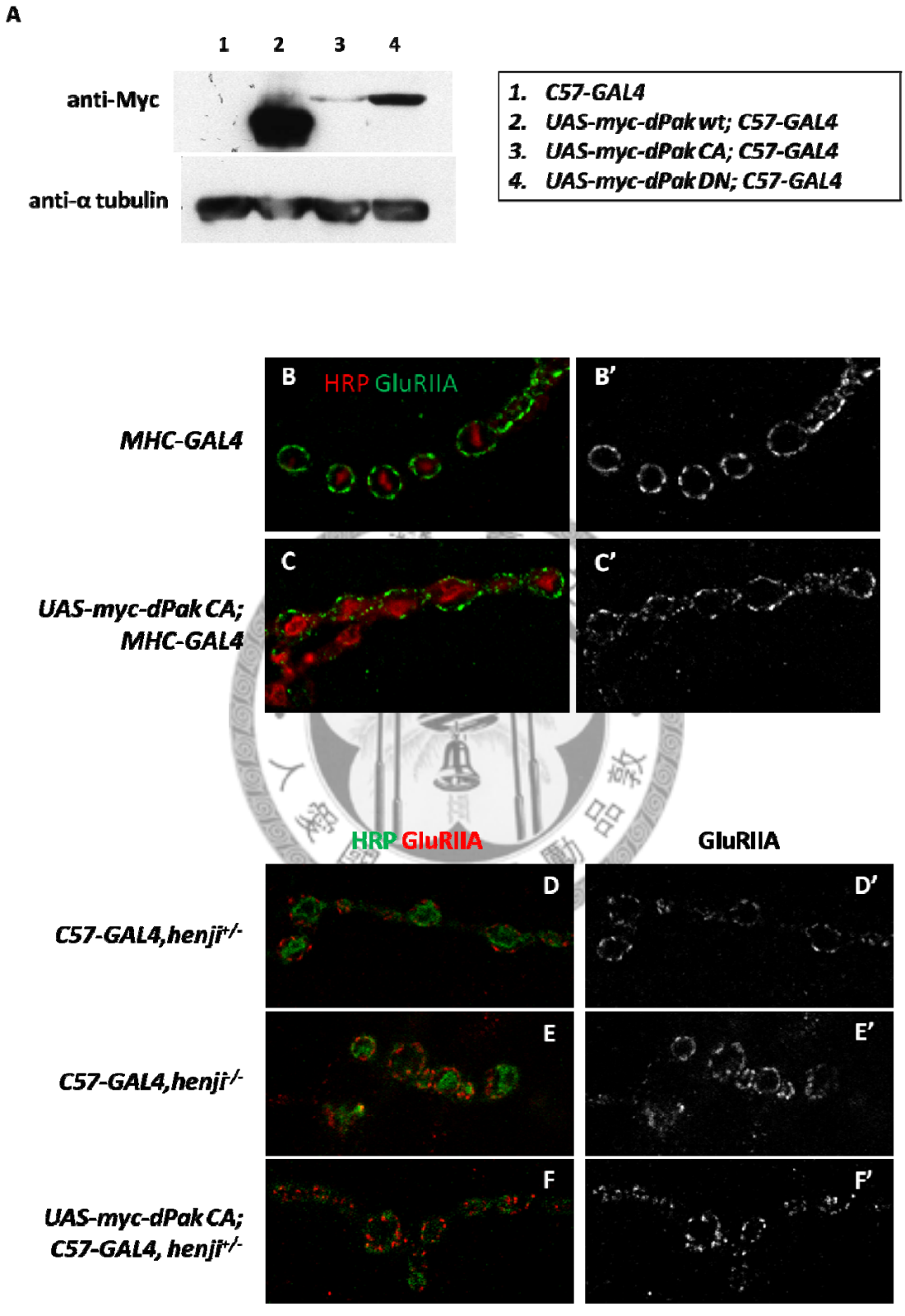
A
1 2 3 4
anti-Myc
anti-α tubulin
1. C57-GAL4
2. UAS-myc-dPak wt; C57-GAL4
3. UAS-myc-dPak CA; C57-GAL4
4. UAS-myc-dPak DN; C57-GAL4
MHC-GAL4
B HRP GluRIIA
B'
UAS-myc-dPak CA; MHC-GAL4
C
C'
HRP GluRIIA
GluRIIA
C57-GAL4,henji+/-
D
D'
C57-GAL4,henji-/-
E
E'
UAS-myc-dPak CA; C57-GAL4, henji+/-
F
F'

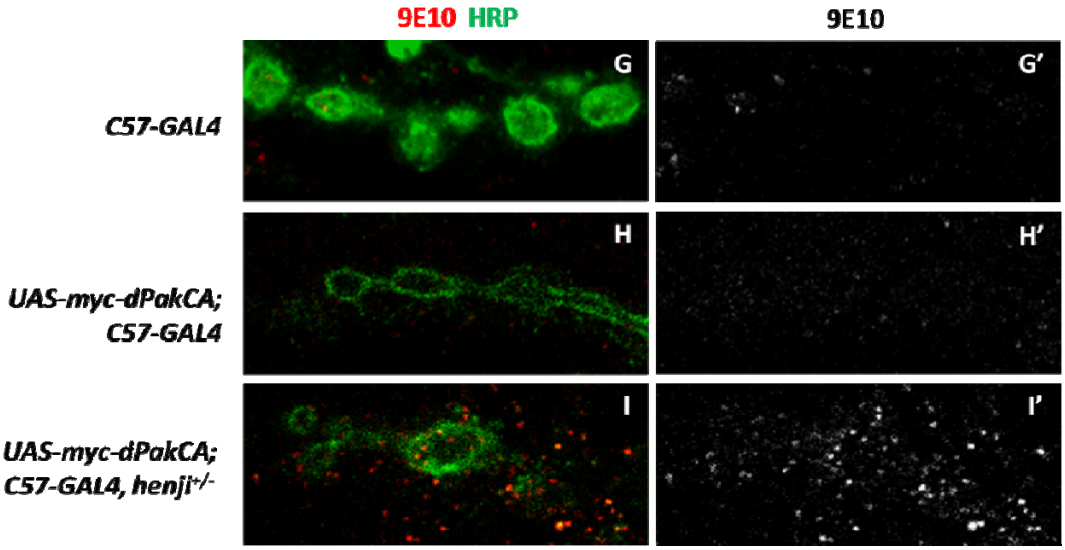

Figure 11. Postsynaptic overexpression of constitutively active form of dPak. (A) Myc-dPak wt, Myc-dPak CA or Myc-dPak DN is overexpressed using the muscle-specific C57-GAL4. Western blotting with 9E10 anti-Myc antibody detects the expression of Myc-dPak CA and Myc-dPak DN proteins. However, Myc-dPAK wt expression is aberrant. The expreriment has been repeated and another muscle-specific MHC-GAL4 was also used. Results from these experiments are similar. Lower panel, anti-α tubulin is used as a loading control. (B-C) GluRIIA abundance at NMJ4 is not altered when Myc-dPak CA is overexpressed in the muscle cell. C57-GAL4 is also tried in this experiment. The results are similar to the ones using MHC-GAL4. (D-F) C57-GAL4, henji2/henji1 (E) has a stronger GluRIIA intensity compared to C57-GAL4, henji2/+ heterozygous control. Postsynaptic overexpression of Myc-dPak CA (F) further enhanced GluRIIA intensity than the *henji* mutant (E). (G-I) NMJ4 labeled with specific

anti-Myc antibodiy 9E10 and HRP. Postsynaptic overexpression of Myc-dPak CA cause an overall elevation of Myc signal in the muscle (compare H to G). Postsynaptic overexpression of Myc-dPak-CA in *henji*$^{+/-}$ mutant background results in enhanced intensity of Myc-positive punctae; in addition, these strongly-stained Myc punctae tend to aggregate around the NMJ, roughly coincide with the region of SSR(subsynaptic reticulum) (I).

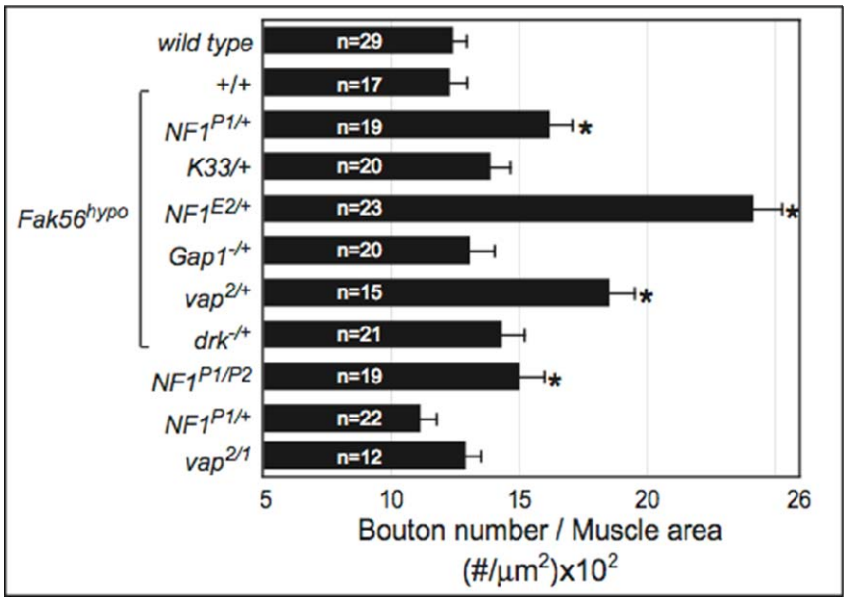

Appendix 1. *Fak56* has strong genetic interactions with *NF1* and *vap*

All three fly *RasGAPs* (*NF1*, *Gap1* and *Vap*) were tested for their genetic interactions with *Fak56*. Heterozygous loss-of-function mutant alleles were introduced into *Fak56* hypomorphic background. Bouton numbers from wandering third instar larvae were counted and normalized to muscle area. Both *NF1* and *Vap* mutants show strong enhancement in bouton numbers compared with *Fak56* hypomorph alone.

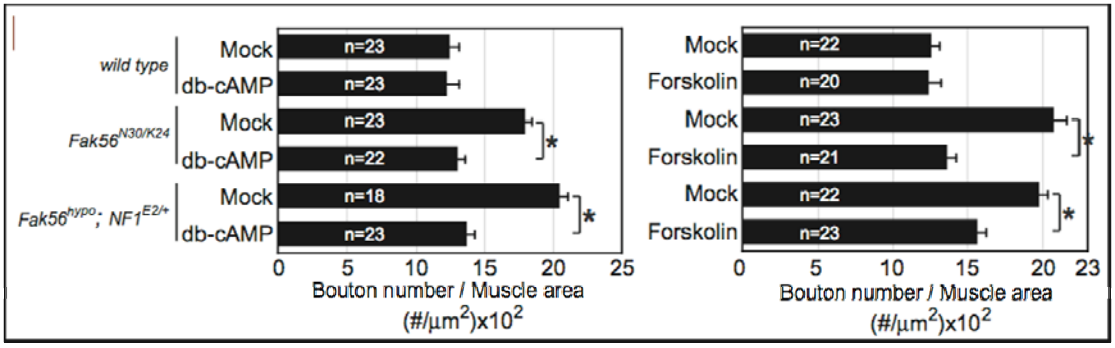

Appendix 2. Fak56 affects bouton addition via cAMP-dependent pathway.

Feeding db-cAMP or forskolin do not alter bouton number in wildtype flies. However, *Fak56* mutant fed with db-cAMP or forskolin show suppressed bouton number as compared with *Fak56* mutant controls fed with water or DMSO.

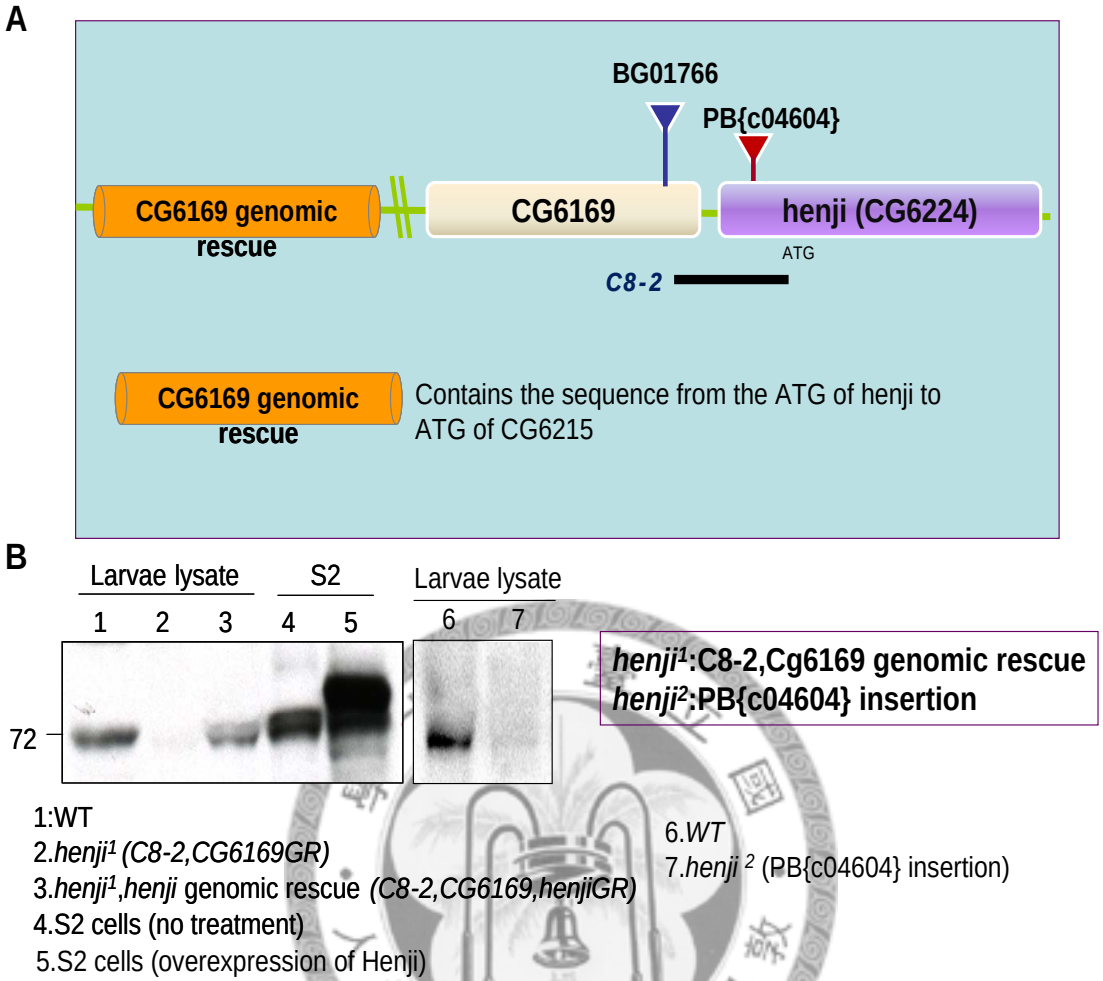

Appendix 3. Characterization of *henji* mutants. (A)Scheme of *Henji* genomic region. Three rectangle represent three genetic loci, *Henj*i (CG6224) in magenta, and the neighboring *CG6169* and *CG6215* in orange and blue. P elements *BG01766* and *PB[c04604]* respectively inserted in the *CG6169* and *CG6224* are marked in blue and red. Deleted chromosomal regions in *C8-2* alleles isolated in this study are shown as black boxes. The 5.2Kb genomic rescue construct is shown below the *CG61659* (the orange cylinder). (B)Western blots of extracts prepared from late-third instar larvae and *Drosophila* S2 cells. The left three lanes show the Henji protein expression, detected by

anti-Henji antibodies, in wild type (lane1), *henji* ^{1}mutant (lane2) *henji* ^{2} mutant (lane7) and genomic rescue flies (lane3). The right lanes show the Henji expression in *Drosophila* S2 cells overexpressing the *UAS-Henji* construct.

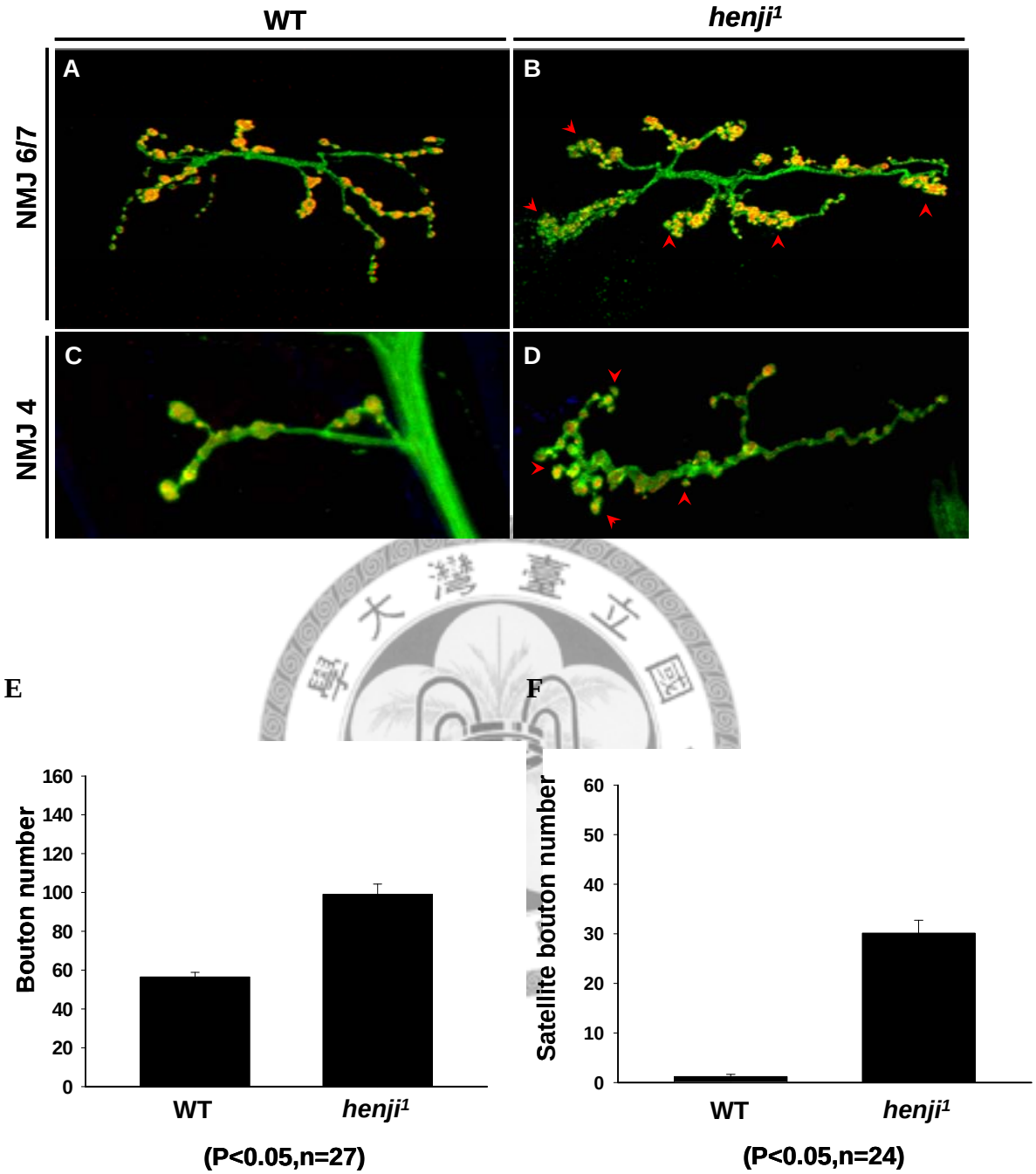

Appendix 4. *henji* mutants show defective NMJ morphology. (A-D) NMJ morphology is altered in *henji* mutants. Third instar NMJ synapses of muscle 6/7 (A and B) and muscle 4 (C and D) are labeled with HRP (green) and synapsin (red) to mark the bouton morphology. Arrowheads point to a clump of satellite boutons. Note that each

satellite bouton contains synapsin immunoreactivity. (E-F) Quantification of the total number of boutons and satellite boutons at muscle 6/7 NMJs of wild type and *henji* mutants (n=24 ,P<0.05).

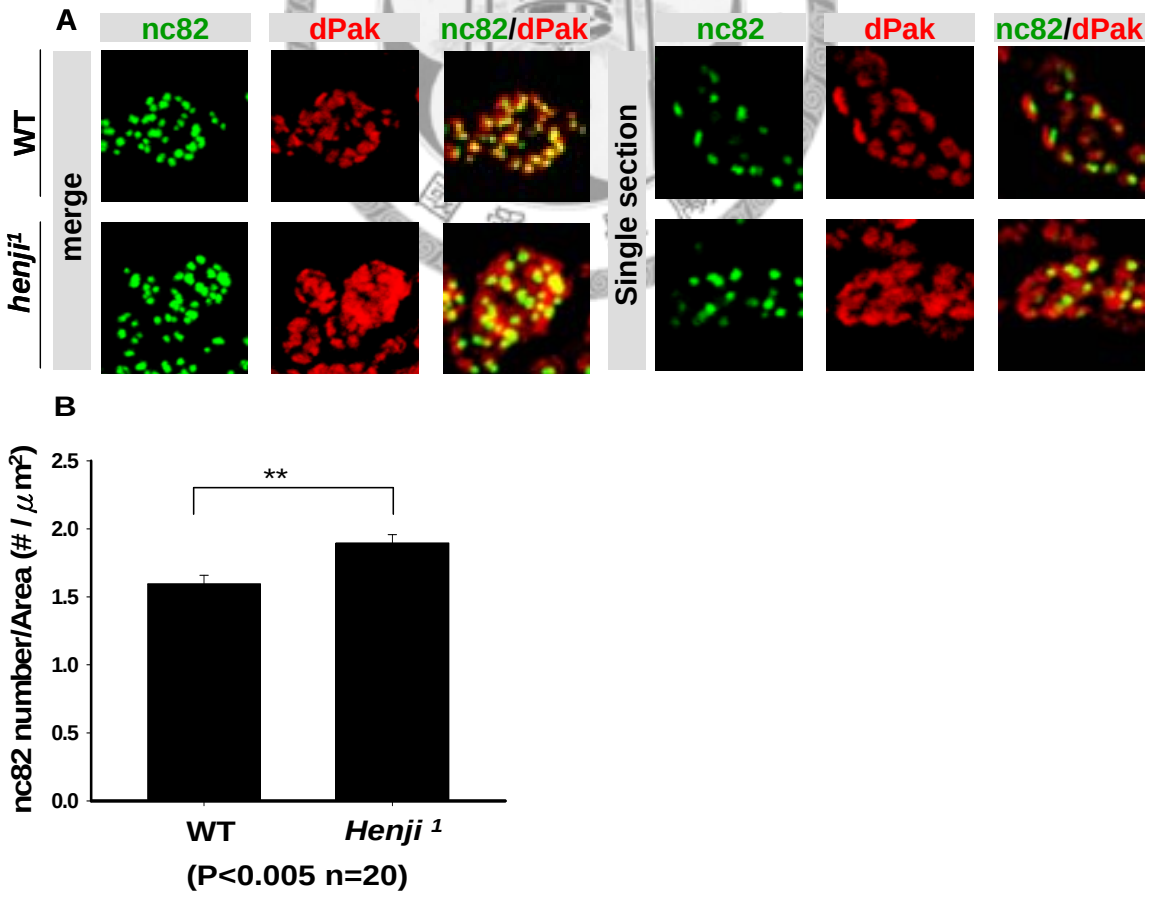

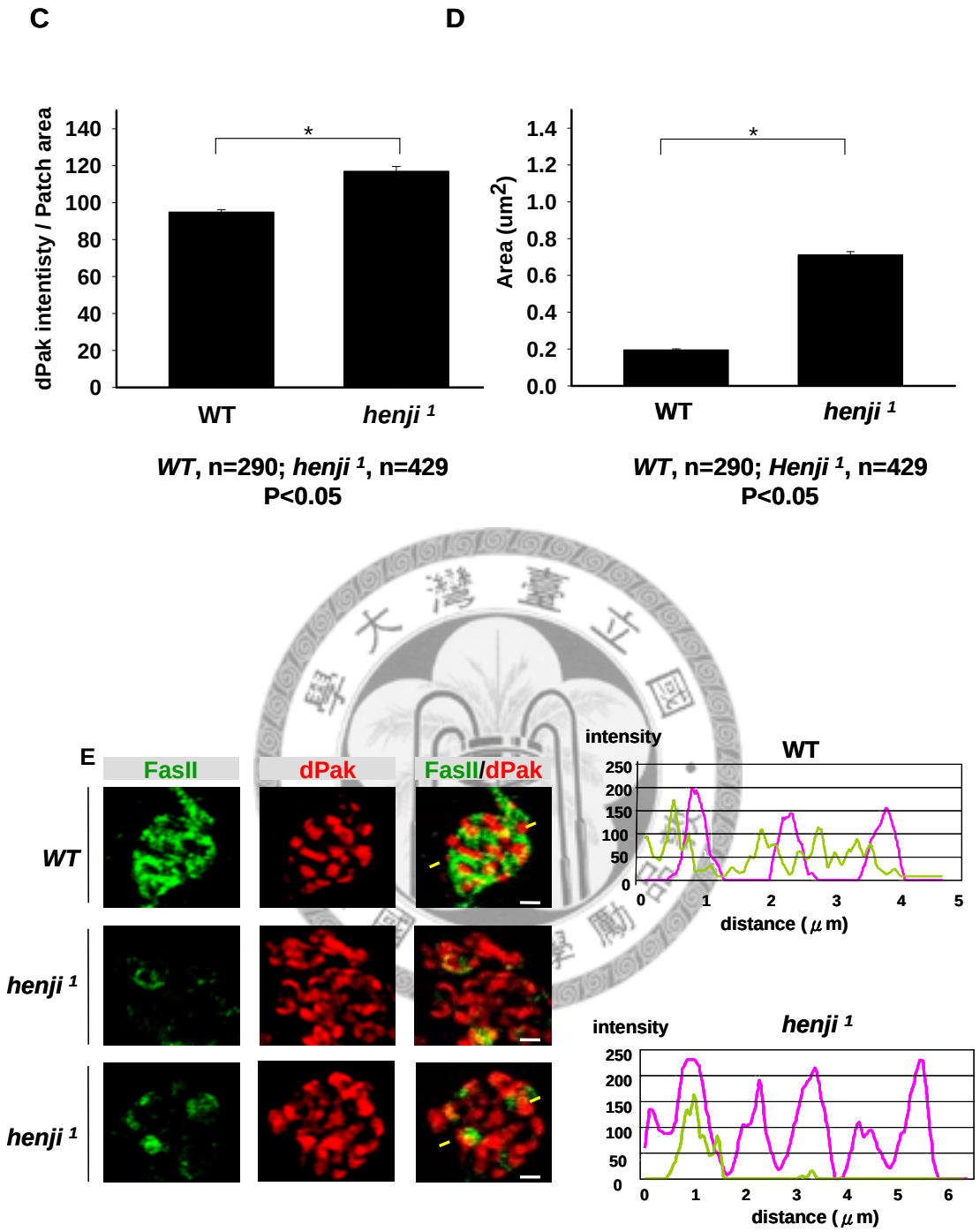

Appendix 5. dPak is dramatically increased but FasII level is decreased in *henji* mutants. (A,E) At wild type third instar larvae NMJ.(A) muscle 4 synapses of mutant and wild type are stained for postsynaptic marker nc82 (green) and dPak(red). The panel

shows the fluorescence of dPak is strongly increased both in the single section or projection. (B-D) Quantification of average active zone number, mean postsynaptic dPak fluorescence intensities and the mean active zone size. dPak signals are adapted from the single section. Mean dPak signals are increased in *henji* mutants by 25% (wild type,n=290; mutant, n=429,$P<0.05$). (E) In wild type, FasII (green) is highly enriched in the perisynaptic membrane but reduced at synaptic membranes. FasII “hole” match the PSD identified via dPak labeling (red). However, in *henji* mutants, atypically homogenous FasII distribution with either no signals or only one small accumulation at dPak sites. (F) Quantification of the FasII (green) and dPak (red) intensity profiles at single section

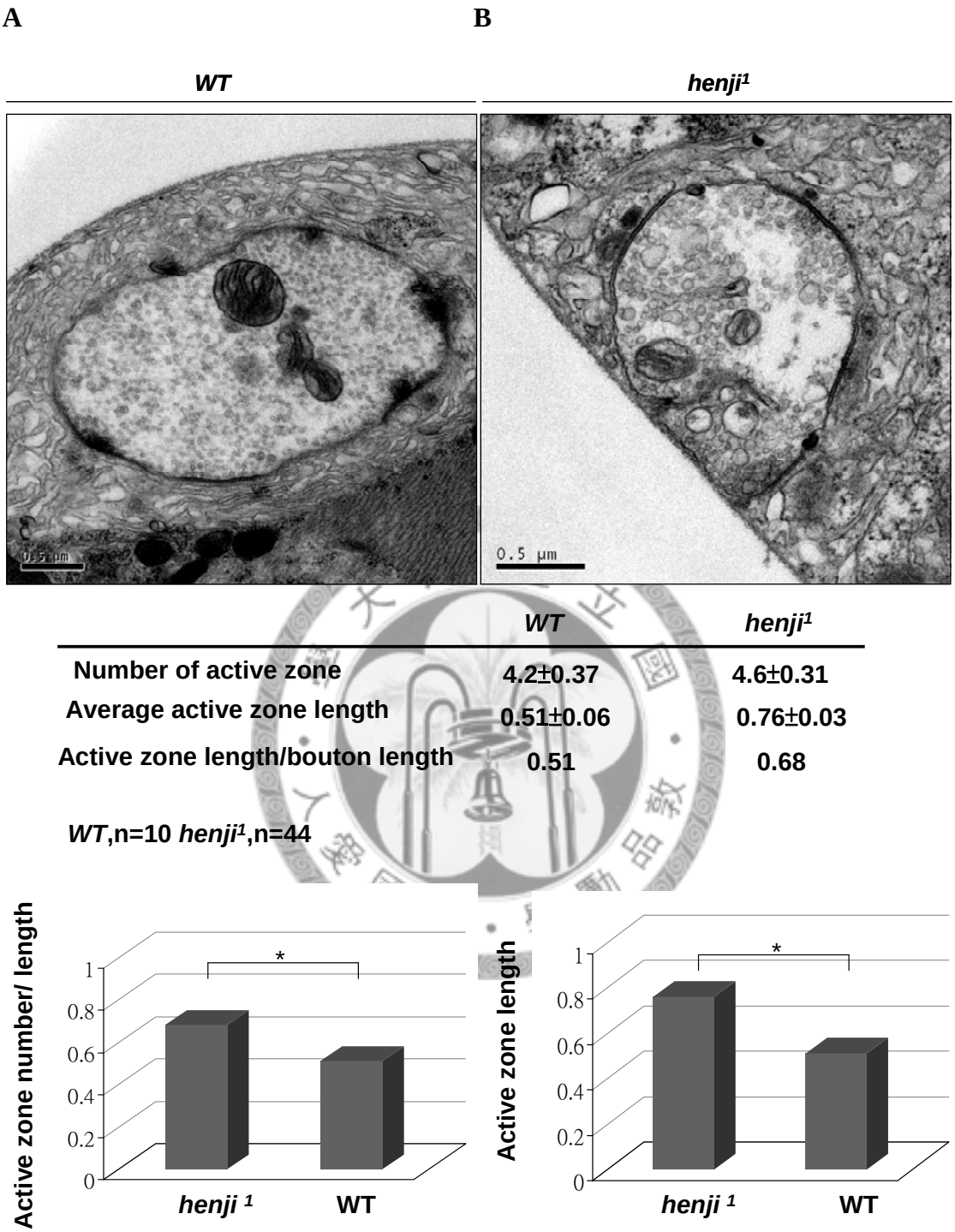

Appendix 6. Ultrastructure of type Ib boutons from NMJs in wild type and mutants. (A-B)TEM of type Ib boutons of NMJs in A2 or A3 segments. Boutons in the mutants exhibit significant enlargement of active zone length. Arrowhead indicates the

active zone and the asterisks show the SSR.

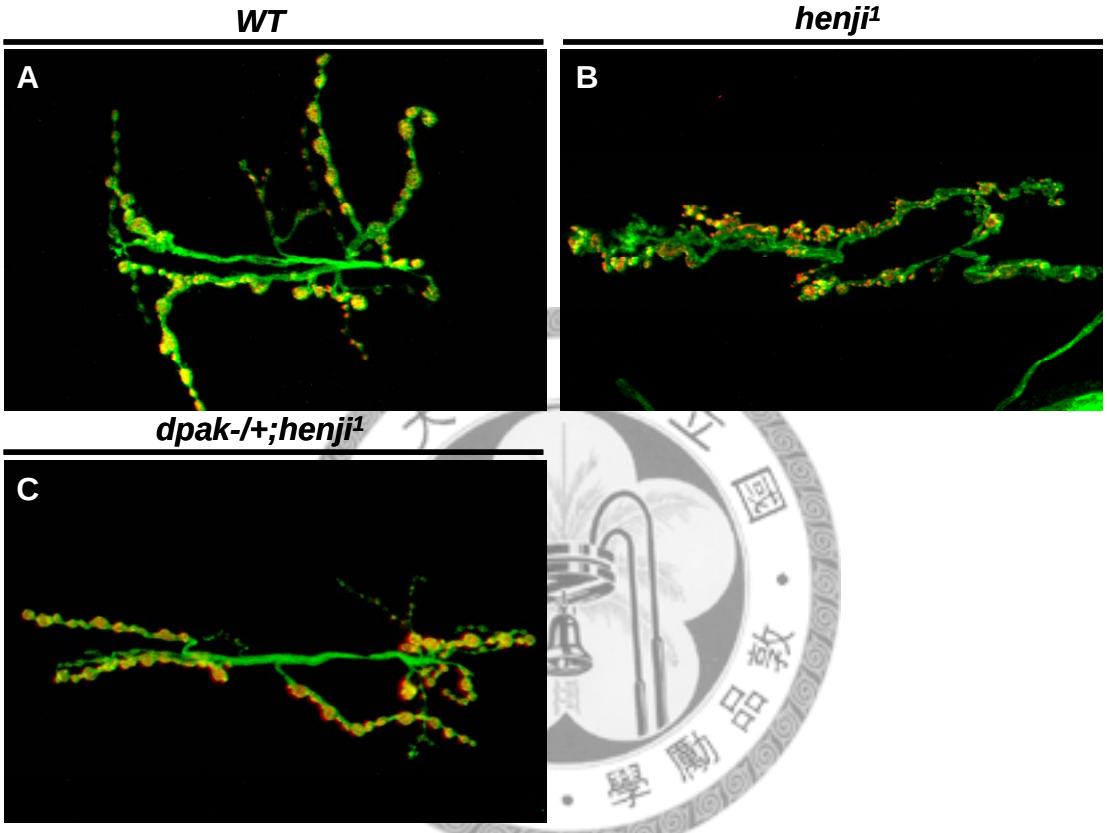

D

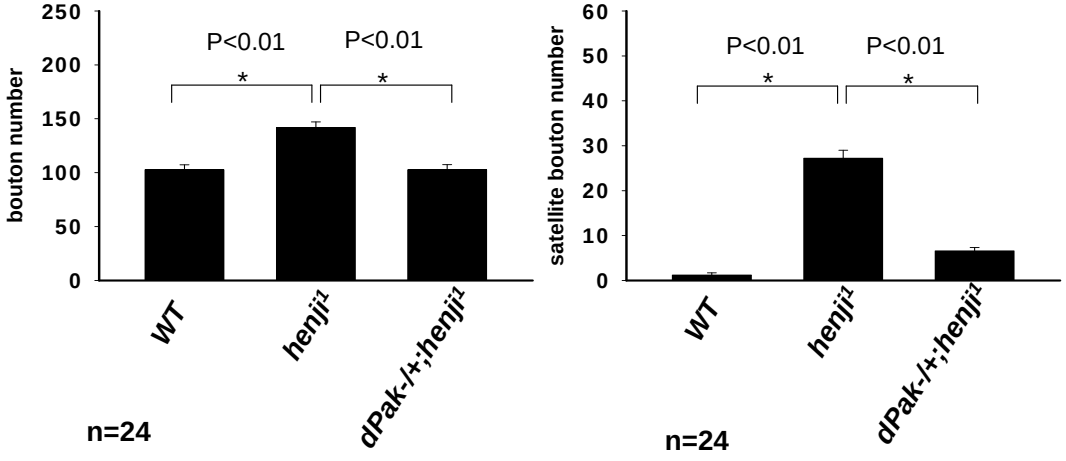

Appendix 7. Henji and dPak interact genetically.

(A~C) NMJ morphology at the muscle 6/7 of the larval muscle segment 2. Quantifications of bouton number in *henji* mutant background by the reduction of dPak gene dosage is shown. Compared to wild type, *henji* mutants have more bouton and satellite boutons. The reduction of *dPak* gene dosage in *henji* mutant can partially reduce the bouton number and satellite bouton numbers compared to *henji* mutants.

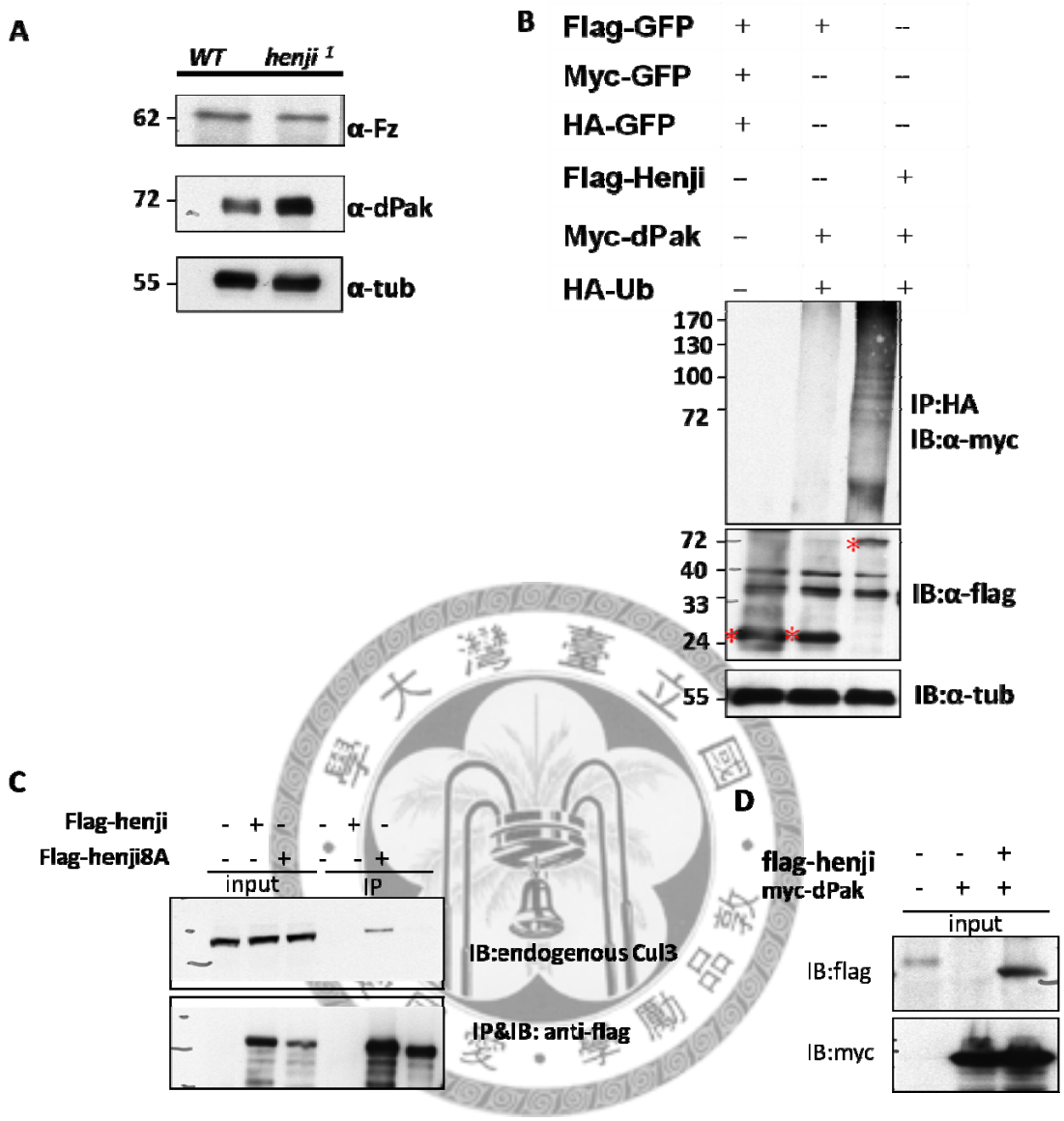

Appendix 8. Impaired ubiquitination and degradation of dPak in henji mutants and henji RNAi knockdown S2 cells. (A) dPak protein levels are increased in *henji* knock-down cells. (B) levels of polyubiquitin-modified dPak were greatly increased by overexpression of Henji. (C) Only in the presence of Henji (lane2) but not Henji 8A(lane3, cullin3 interaction deficient mutants) , the endogenous cullin3 was immunoprecipitated (D) Henji proteins can be pulled down in the presence of myc-dPak.

A

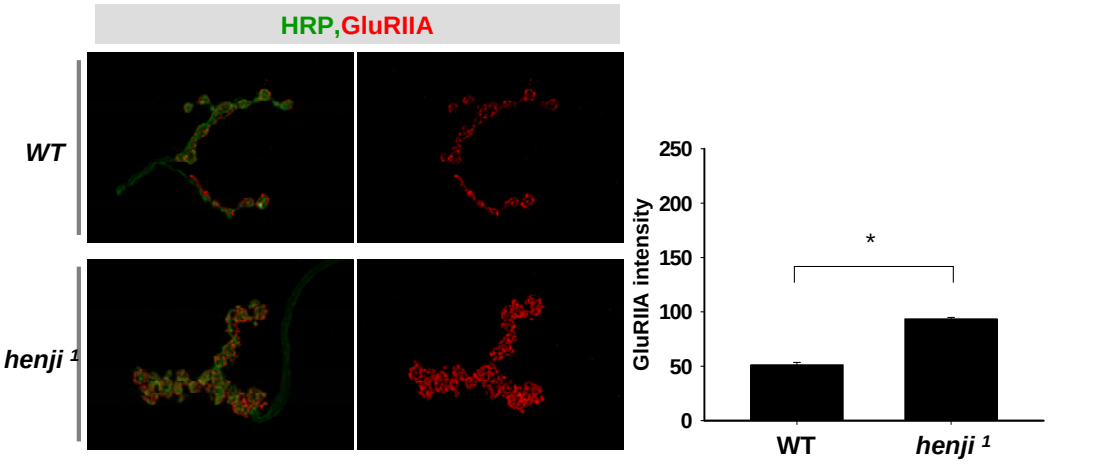

P<0.05, WT,n=168, *henji 1*,*n=803*

B

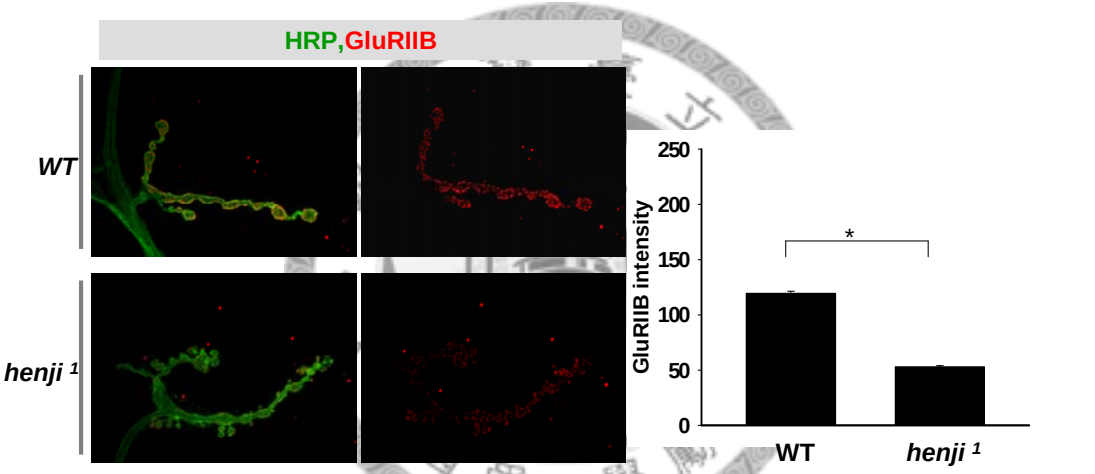

P<0.05, WT,n=295, *henji 1*,*n=549*

C

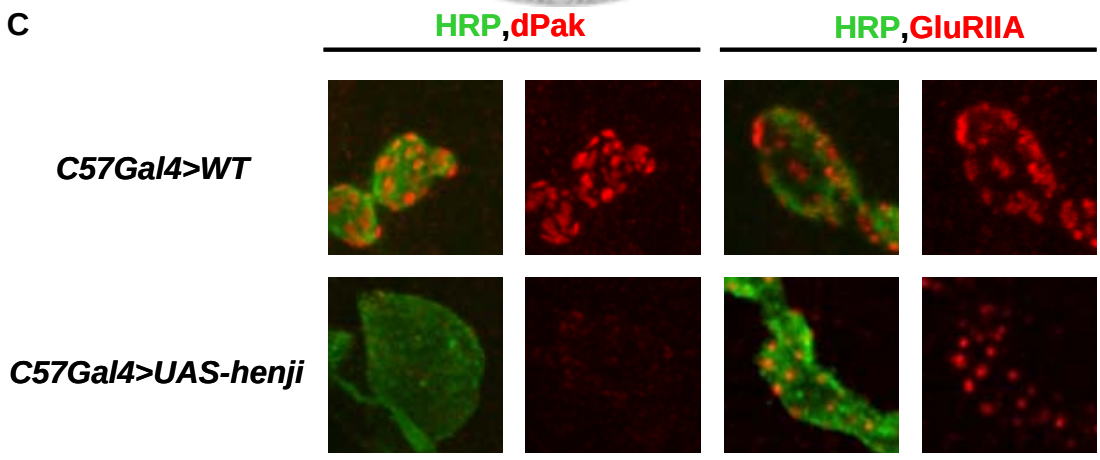

Appendix 9. GluRIIA intensity is increased but GluRIIB intensity is decreased in *henji* mutants. (A and B) Representative NMJ in *wild type* and *henji*^{1} mutants are shown that are respectively costained with anti-GluRIIA or anti-GluRIIB and anti-HRP. At the henji mutant NMJ, synaptic GluRIIA abundance is substantially increased. However, the GluRIIB abundance is decreased. The quantification of the average fluorescence intensity of GluRIIA and GluRIIB are shown. There is a statistically significant changes in GLuRIIA and GluRIIB fluorescence intensity in *henji* mutants. (C) In the muscle overexpression of Henji, the dPak level is decreased compared to C57-GAL4 controls. In addition, the size and the intensity of GluRIIA are decreased in *henji* mutants.

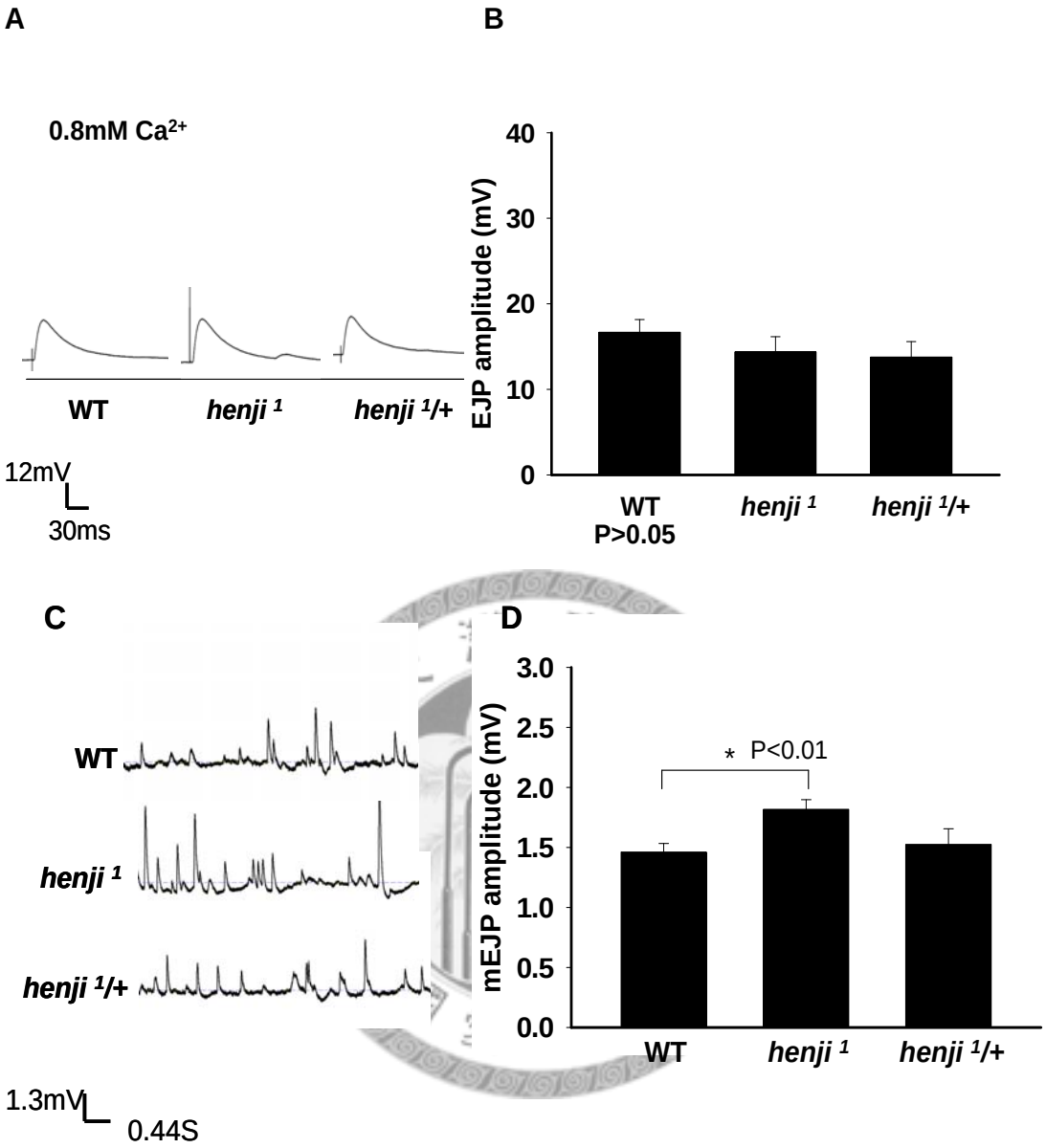
A
B
0.8mM Ca2+
WT
henji 1
henji 1/+
12mV
30ms
EJP amplitude (mV)
40
30
20
10
0
WT
henji 1
henji 1/+
P>0.05
C
D
WT
henji 1
henji 1/+
1.3mV
0.44S
mEJP amplitude (mV)
3.0
2.5
2.0
1.5
1.0
0.5
0.0
* P<0.01
WT
henji 1
henji 1/+
E
F
Frequency (Hz)
5
4
3
2
1
0
WT
henji 1
henji 1/+
Quantal content
25
20
15
10
5
0
* P<0.05
WT
henji 1
henji 1/+

Appendix 10. Evoked release but not spontaneous release is normal in *henji* mutant. (A-B) Sample EJPs and quantification of their amplitude for wild type and *henji* mutants in 0.8mM Ca^{2+}.(B) mutants do not show a significant difference in EJP amplitude in 0.8 mM Ca^{2+}. (C-D) Sample mEJP traces of wild type and *henji* mutants. The mEJP amplitude of *henji* mutants is increased compared to the wild type whereas the mEJP frequency is not altered (E). (F) The quantal content is estimated by the ratio of EJP/mEJP. There are statistically significant changes of quantal content in mutants.

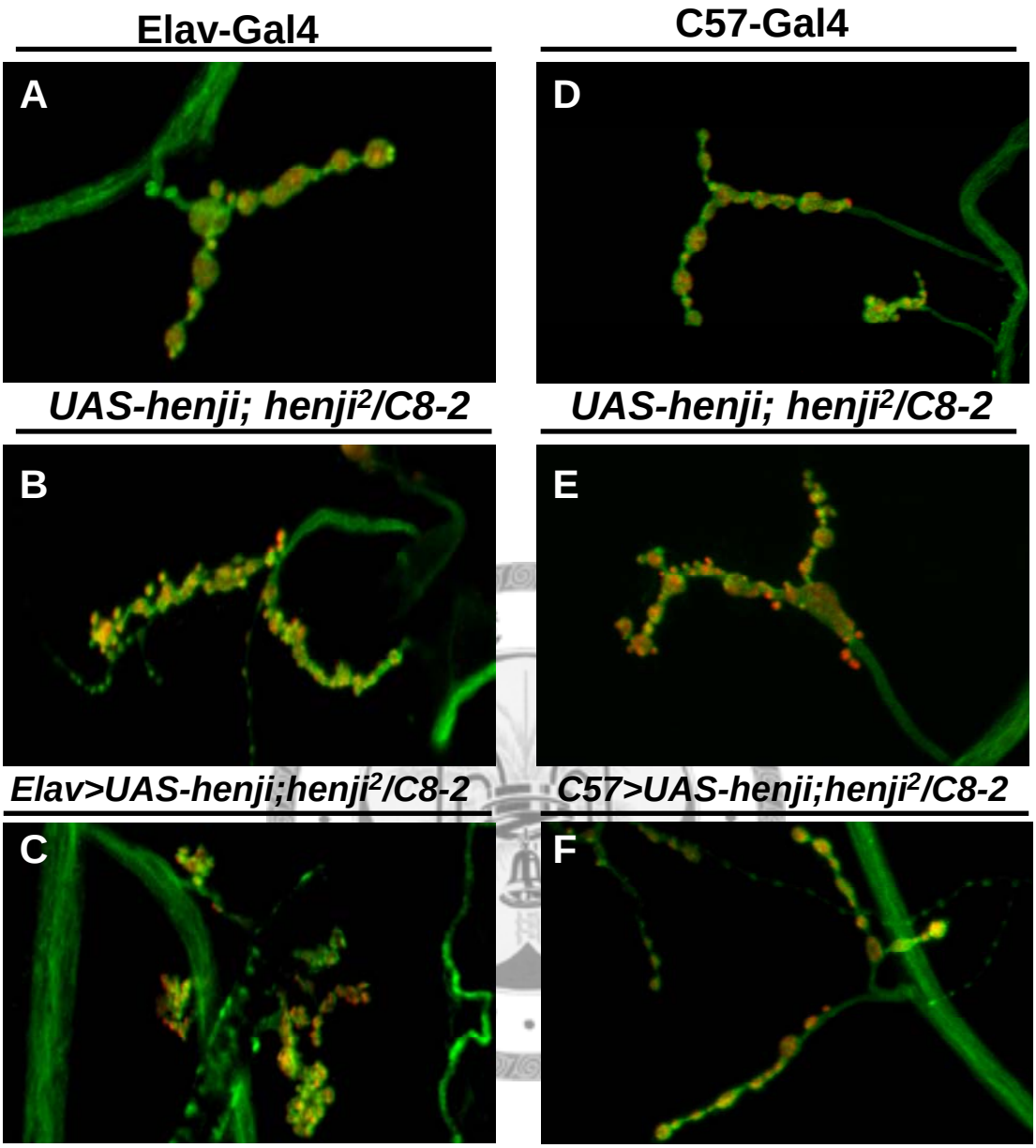

Appendix 11. Muscle expression of Henji can rescue the satellite phenotype. (A~F) NMJ morphology at muscle4 of larval abnorminal segment2 label with anti HRP and synapsin. Compared to elav-GAL4 and C57-GAL4(A andD), UAS-henji;henji mutants (B and E) have more satellite boutons. A rescue with muscle expression of *UAS-henji* cDNA in *henji*^{2}*/C8-2* background appears to restore NMJ morphology.